International Journal of Bifurcation and Chaos, Vol. 30, No. 14 (2020) 2030040 (29 pages)

DOI: 10.1142/S0218127420300402

Milnor and Topological Attractors in a Family of Two-Dimensional Lotka–Volterra Maps

Laura Gardini*
Department DESP,
University of Urbino, Italy
laura.gardini@uniurb.it

Wirot Tikjha
Faculty of Science and Technology,
Pibulsongkram Rajabhat University,
Phitsanulok 65000, Thailand
Centre of Excellence in Mathematics,
PERDO, CHE, Thailand
wirottik@psru.ac.th

Received March 26, 2020

In this work, we consider a family of Lotka–Volterra maps $(x', y') = (x(a - x - y), bxy)$ for $a > 1$ and $b > 0$ which unfold a map originally proposed by Sharkosky for $a = 4$ and $b = 1$. Multistability is observed, and attractors may exist not only in the positive quadrant of the plane, but also in the region $y < 0$. Some properties and bifurcations are described. The x-axis is invariant, on which the map reduces to the logistic. For any $a > 1$ an interval of values for b exists for which all the cycles on the x-axis are transversely attracting. This invariant set is the source of several kinds of bifurcations. Riddling bifurcations lead to attractors in Milnor sense, not topological but with a stable set of positive measure, which may be the unique attracting set, or coexisting with other topological attractors. The riddling and blowout bifurcations are described related to chaotic intervals on the invariant set, and these global bifurcations have different dynamic results. Chaotic intervals which are not topological attractors may have all the cycles transversely attracting and as Milnor attractors. We show that Milnor attractors may also be related to attracting cycles on the x-axis at the bifurcation associated with the transverse and parallel eigenvalues. We show particular examples related to topological attractors with very narrow basins of attraction, when the majority of the trajectories are divergent.

Keywords: Lotka–Volterra family; noninvertible map; Milnor attractor; homoclinic bifurcation; riddling bifurcation; blowout bifurcation.

1. Introduction

Since the celebrated paper by Milnor [1985] focusing on the existence of invariant sets which are not attractors in the Lyapunov sense, but may attract a set of points of positive measure, many papers have been published dealing with this kind of invariant sets, also called nontopological Milnor attractors. In particular, this notion has been widely used in the study of systems in discrete time with symmetries, having an invariant set on which the restriction is a lower-dimensional map and to which trajectories may converge even if there is not a topological attractor on it. This kind of studies also gave rise to the investigation of new kind of global bifurcations,

*Author for correspondence

called riddling bifurcations and blowout bifurcations [Ashwin *et al.*, 1996; Lai & Grebogi, 1996; Buescu, 1997; Nagai & Lai, 1997; Viana & Grebogi, 2001] to cite a few. In symmetric maps the synchronization phenomena, in particular chaos synchronization achieved in the long run, has been investigated by many authors, especially for the intermittency phenomena [Pecora & Carroll, 1990, 2015; Alexander *et al.*, 1992; Ott & Sommerer, 1994; Maistrenko *et al.*, 1998; Viana *et al.*, 2003].

Less studied are these dynamic behaviors in systems described by nonsymmetric maps, in which some invariant set exists, related to a lower-dimensional map. For example, the generalized two-dimensional Lotka–Volterra maps of the kind $(x', y') = (xF(x, y), yG(x))$, having the x-axis invariant and on which the restriction of the map reduces to $x' = xF(x, 0)$.

In this work, we consider the particular family of Lotka–Volterra maps $(x', y') = T(x, y)$ given by

$$T(x,y) := \begin{cases} x' = x(a - x - y), \\ y' = bxy, \end{cases} \tag{1}$$

where the parameters a, b are real numbers subject to $a > 1$ and $b > 0$.

This system has been investigated by many authors in the particular case $(a, b) = (4, 1)$ proposed by Sharkovsky [1993], see e.g. [Swirszcz, 1998; Balibrea *et al.*, 2006; Guirao & Lampart, 2008; Malicky, 2012; Gasull & Mañosa, 2020]. For such values of the parameters the map is chaotic in the triangle Δ bounded by the segments $[0, a]$ on the axes of the phase plane (x, y) and the diagonal connecting $(0, a) - (a, 0)$. Also in this particular case, there are still properties not completely proved. A first unfolding of the particular case at fixed parameter values has been considered in [Gardini & Tikjha, 2020], for $b = 1$ and $a > 1$. In that paper, previous results related to $(a, b) = (4, 1)$ are recalled and the transitions to chaotic behaviors for $1 < a < 4$ via snap-back repeller bifurcations of many cycles are commented. Moreover, some properties in the case $b = 1$ were left not proved, for example, the nonexistence of 2-cycles internal to Δ, which can be proved now with the unfolding here considered, with $b > 0$.

As already mentioned, map T is invariant on the line $y = 0$, and the restriction is the one-dimensional map $f(x) = x(a - x)$ which is topologically conjugate to the standard logistic map $g(x) = ax(1-x)$ since we have $h^{-1} \circ f \circ h(x) = g(x)$ with the conjugacy $h(x) = ax$.

As a Lotka–Volterra map, the interest of the dynamics of map T may be mainly in attractors belonging to the positive quadrant, in particular internal to the triangle Δ, and indeed we shall prove that for a wide range of parameters' values this set is mapped into itself, $T(\Delta) \subset \Delta$. But in the unfolded range $b > 0$ cycles not belonging to the x-axis may exist also external to Δ. Moreover, we shall prove the existence of several regimes in which the trajectories are attracted to the x-axis, either to a topological attractor or to a Milnor attractor, which may be the unique one or coexisting with some other attractor.

From [Milnor, 1985], a Milnor attractor may be a topological one or nontopological, but for the sake of clarity we prefer to use different terms for the two different cases, so let us give a few definitions that are used in the present work.

Definitions. Let $\mathcal{A}$ be a *compact invariant set* (i.e. such that $T(\mathcal{A}) = \mathcal{A}$).

(i) The *stable set* of $\mathcal{A}$, $W^S(\mathcal{A})$, consists of the points (x, y) whose ω-limit set satisfies $\omega(x, y) \subseteq \mathcal{A}$.

(ii) $\mathcal{A}$ is a *topological attractor* (or asymptotically stable or Lyapunov stable) if for any neighborhood $V(\mathcal{A})$ an open neighborhood $U(\mathcal{A})$ exists, $\mathcal{A} \subset U(\mathcal{A}) \subset V(\mathcal{A})$, such that for any $(x, y) \in U(\mathcal{A})$, it is $T^n(x, y) \in V(\mathcal{A})$ for any n and $\omega(x, y) \subseteq \mathcal{A}$, and it does not exist for any compact subset $\mathcal{A}' \subset \mathcal{A}$ with the same property.

(iii) For a topological attractor the stable set $W^S(\mathcal{A})$ (which includes an open neighborhood of $\mathcal{A}$) is also called *basin of attraction*, and denoted $B(\mathcal{A})$.

(iv) We say that $\mathcal{A}$ is a *Milnor attractor* when it is not a topological attractor and $W^S(\mathcal{A})$ is a set of positive Lebesgue measure.

Map T may have topological attractors internal to Δ, external to Δ or belonging to the x-axis, and in particular we shall investigate those belonging to the x-axis, since belonging to an invariant set these may have particular transverse bifurcations, and may be topological or Milnor attractors.

It is plain that for a topological attractor the global basin of attraction can also be defined via $B(\mathcal{A}) = U_{n=0}^{\infty} T^{-n}(U(\mathcal{A}))$, while it is more difficult to detect the stable set of a Milnor attractor belonging to the invariant x-axis, and we shall mainly use numerical evidence for this. Moreover, we have to

mention the techniques which have been used in the literature, especially when the invariant set of the one-dimensional map consists of chaotic intervals [Ashwin *et al.*, 1996; Buescu, 1997].

For any point $(x, 0)$ of the invariant line we have two eigenvalues, one related to the eigenvector along the x-axis, $\lambda_{\parallel}(x)$, and one related to the eigenvector transverse to it, $\lambda_{\perp}(x)$. The *transverse Lyapunov exponent* related to the orbit $\{x_i = f^i(x_0),\ i \geq 0\}$ of a point x_0 for the one-dimensional map $f(x)$ is defined by

$$\Lambda_{\perp} = \lim_{N\to\infty} \frac{1}{N} \sum_{i=0}^{N} \ln|\lambda_{\perp}(x_i)|. \tag{2}$$

Clearly, for a point x_0 of a k-cycle of $f(x)$ this leads to $\Lambda_{\perp}(x_0) = \ln|\prod_{i=0}^{k-1} \lambda_{\perp}(x_i)|$ and the k-cycle is transversely attracting for $\Lambda_{\perp}(x_0) < 0$. This definition becomes particularly relevant when it is associated with an invariant attracting set $\mathcal{A}$ on the x-axis consisting of chaotic intervals. In that case, the periodic orbits are dense in $\mathcal{A}$ but the generic trajectory is aperiodic and dense in $\mathcal{A}$. Thus, considering a generic point x_0 (neither periodic nor preperiodic) the associated exponent $\Lambda_{\perp}$ is the so-called *natural transverse Lyapunov exponent*, which represents the average transverse attractiveness of the chaotic set $\mathcal{A}$. It is relevant especially when the invariant set on the restriction has a natural transverse parameter, that is, a parameter which influences only the transverse eigenvalue, as we shall see to be the parameter b in our system.

Considering the system as a function of the transverse parameter we can define a spectrum of transverse Lyapunov exponents [Ashwin *et al.*, 1996; Buescu, 1997], in our case as a function of b:

$$\Lambda_{\perp}^{\min} < \cdots \Lambda_{\perp}^{\text{nat}} < \cdots < \Lambda_{\perp}^{\max}. \tag{3}$$

When all the cycles of $\mathcal{A}$ are transversely attracting, then it is $\Lambda_{\perp}^{\max} < 0$ and the invariant set $\mathcal{A}$ may be a topological attractor for the two-dimensional map T, it is so if a neighborhood exists as in the definition given above. When, varying b, one cycle becomes transversely repelling then we have the transition from $\Lambda_{\perp}^{\max} < 0$ to $\Lambda_{\perp}^{\max} > 0$ which causes the transition to a Milnor attractor $\mathcal{A}$. In fact, the invariant set is no longer an attractor, because an open neighborhood belonging to its basin of attraction no longer exists. This is due to the property that all the cycles in the invariant chaotic intervals have preimages which are dense in the chaotic intervals, which implies that the unstable branches issuing transversely from the cycle have also infinitely many unstable branches issuing from the dense preimages. It follows that for any point $(x, 0)$ belonging to the chaotic intervals it holds that in any neighborhood of $(x, 0)$ there are points with unstable branches issuing from the neighborhood. However, there are still infinitely many other saddle cycles in the chaotic intervals which are transversely attracting, and for each of them it is also true that there are infinitely many preimages dense in the chaotic intervals. This influences the global behavior, because when on average such transversely attracting cycles are dominating, and occurs for $\Lambda_{\perp}^{\text{nat}} < 0$, then the invariant chaotic intervals have a stable set of positive measure, numerically and experimentally observable, and this leads to a Milnor attractor $\mathcal{A}$. Notice that this stable set $W^S(\mathcal{A})$ does not include any open set, because for any point $(x, y) \in W^S(\mathcal{A})$ it holds that in any open neighborhood of the point there are points not converging to $\mathcal{A}$, and in order to identify such a behavior, the term *riddled basin* was introduced, whose meaning is exactly the nonexistence of open sets in the stable set. That is, the stable set of a Milnor attractor may be a kind of "basin riddled in something else" [Alexander *et al.*, 1992; Lai & Grebogi, 1996; Lai *et al.*, 1996; Buescu, 1997]. This is especially observed when the system has, besides $\mathcal{A}$, a coexisting attracting set and the transition of $\mathcal{A}$ from topological attractor to Milnor attractor is also called *riddling bifurcation*. But, as we shall see, a different attracting set may also not exist, in which case the riddling phenomenon is not observed.

As long as $\Lambda_{\perp}^{\text{nat}} < 0$ is a function of the transverse parameter b, on average, the cycles in the chaotic intervals still have dominating transversely attracting eigenvalues, and $\mathcal{A}$ persists as Milnor attractor. The so-called *blowout bifurcation* occurs when the natural transverse Lyapunov exponent $\Lambda_{\perp}^{\text{nat}}$ from negative becomes positive, which means that in the chaotic intervals the cycles which are transversely repelling are dominating [Nagai & Lai, 1997]. Although many transversely attracting cycles may still exist, the stable set of $\mathcal{A}$ becomes a set of zero Lebesgue measure in the (x, y)-plane. When all the cycles in the chaotic intervals are transversely repelling, leading to $\Lambda_{\perp}^{\min} > 0$, then $\mathcal{A}$ becomes fully transversely repelling, and it is also called a *chaotic saddle*.

We shall see different examples of riddled basins and blowout bifurcations associated with attractors consisting of chaotic intervals on the x-axis, but not only. In fact, Milnor attractors may be related also to the transverse bifurcations of cycles, or to the parallel eigenvalue, and we shall see several examples.

Moreover, in [Gardini & Tikjha, 2020] is shown the existence of infinitely many intervals (for the parameter a) in which the so-called maximal cycles with symbolic sequence RL^n on the x-axis (having the largest number of periodic points on the left side of the critical point) are topological attractors of map T. As we shall see, this implies that these cycles become transversely repelling for $b > 1$, when Δ is shown to be no longer mapped into itself. Instead, the majority of the points in the positive quadrant as well as in Δ have divergent trajectories, and despite this, it is possible to have also coexistence of topological attractors for T.

After this Introduction, some properties of map T are described in Sec. 2. We determine the bifurcations of the fixed points of the map, and of the 2-cycles, among which is the one not belonging to the x-axis, showing that it is associated with a subcritical flip bifurcation of the internal fixed point and that it does not exist for $b = 1$. It is proved that the stable set of the origin is particular, and belongs to the boundary of the basin of divergent trajectories. We show that for any $a > 1$ an interval of values for b exists for which all the cycles on the x-axis are transversely attracting. Thus, an attracting set for $f(x)$ on the x-axis is a topological attractor also for map T, and some bifurcation scenarios are commented on. In Sec. 3, we consider the invariant set $\mathcal{A}$ as chaotic intervals on the x-axis both when it is a topological attractor and when it is not, since a set of chaotic intervals may have all the cycles transversely attracting without being a topological attractor. We describe, via numerical simulations, the riddling bifurcations and the blowout bifurcations in different cases, all of which have some peculiar behavior. As we shall see, after a riddling bifurcation it is possible that almost all the points in the triangle Δ are attracted to the Milnor attractor on the x-axis. Section 4 deals with topological attracting cycles on the x-axis, which may become Milnor attractors at the bifurcation related to the transverse eigenvalue, and in some cases the Milnor attractors persist for an interval of values of b. Particular behaviors are numerically observed when the topological attractors are the maximal cycles with symbolic sequence RL^n on the x-axis, for $n \geq 2$. We show that also when the largest part of the points in Δ have divergent trajectories, topological attractors of map T exist and Milnor attractors at the bifurcation related to the transverse eigenvalue may be observed. Some conclusions are given in Sec. 6.

2. Some Properties and Bifurcations of Map T

Map T in (1) has three fixed points, with two of the restrictions on the axis $y = 0$, the origin O and P_0, and P^* in the region $x > 0$ which may belong to the positive quadrant:

$$O := (0, 0), \quad P_0 := (a - 1, 0),$$
$$P^* := (x^*, y^*) = \left(\frac{1}{b}, a - 1 - \frac{1}{b}\right). \tag{4}$$

Map T is noninvertible and its inverses, say $T^{-1}(u, v)$, can be obtained by solving the system

$$\begin{cases} u = x(a - x - y), \\ v = bxy, \end{cases}$$

to get the values for (x, y). Let (u, v) satisfy

$$D(u, v) = \left(\frac{a}{2}\right)^2 - \left(u + \frac{v}{b}\right) \geq 0 \tag{5}$$

then we have two inverse functions of T, leading to points on opposite sides of the critical line LC_{-1} (following the notation introduced in [Mira, 1987; Mira *et al.*, 1996]) of equation $x = \frac{a}{2}$ (denoted as L and R for short), given by

$$T^{-1}_{L/R}(u, v) = (x_{L/R}, y_{L/R})$$
$$= \left(\frac{a}{2} \mp \sqrt{\left(\frac{a}{2}\right)^2 - \left(u + \frac{v}{b}\right)}, \frac{v}{bx_{L/R}}\right). \tag{6}$$

Clearly, the set of points (x, y) satisfying $D(x, y) = 0$ corresponds to the critical curve LC of map T, whose Cartesian equation is given by $y = b\left(\frac{a^2}{4} - x\right)$:

$$\mathrm{LC}_{-1}: \ x = \frac{a}{2}, \quad \mathrm{LC}: \ y = b\left(\frac{a^2}{4} - x\right). \tag{7}$$

In particular, the preimage of P^* different from itself under T is $P^{*,-1} = (a - \frac{1}{b}, \frac{1}{b} - \frac{1}{ab-1})$, while the preimage of P_0 different from itself under T is

the point $P_0^{-1} = (1, 0)$, which is independent of the values of the parameters.

The Jacobian matrix of map T is given by

$$J_T(x, y) = \begin{bmatrix} a - 2x - y & -x \\ by & bx \end{bmatrix} \tag{8}$$

leading to

$$\begin{aligned} \mathrm{Tr}(J_T) &= a - 2x - y + bx, \\ \det(J_T) &= bx(a - 2x). \end{aligned} \tag{9}$$

The critical lines of map T separating zones of points having a different number of preimages satisfy $\det(J_T) = 0$, so that we have $x = 0$ and $x = \frac{a}{2}$. However, the y-axis is mapped into one point, the origin O, a property of the fixed point O of map (1) which holds for any value of the parameters for $b \neq 0$, and thus it is not a separator of zones (since that property implies that O is a focal point of the inverse map with prefocal line the y-axis, as remarked in [Bischi *et al.*, 1999]). The only critical line LC_{-1} is the one evidenced above, $x = \frac{a}{2}$, and it is mapped into LC. In fact $T(\frac{a}{2}, t) = (\frac{a^2}{4} - \frac{a}{2}t, b\frac{a}{2}t)$, and eliminating the parameter t we get Eq. (7), but its role (and definition) is due to the fact that any point $(x, y) \in \mathrm{LC}$ has two preimages merging into one point of LC_{-1} as immediately from the inverses in (6). The point $\mathrm{LC} \cap \mathrm{LC}_{-1}$ is given by $\left(\frac{a}{2}, \frac{ab}{4}(a - 2)\right)$.

For a point of the x-axis on the Jacobian matrix is upper triangular, so that from $J_T(x, 0)$ we have immediately the eigenvalues parallel and transverse to the x-axis:

$$\lambda_{\parallel}(x) = a - 2x, \quad \lambda_{\perp}(x) = bx \tag{10}$$

and for an n-cycle on the x-axis with periodic points $\{x_1, \ldots, x_n\}$, which are necessarily all positive, the eigenvalues are given by:

$$\lambda_{n,\parallel} = \prod_{i=1}^{n}(a - 2x_i), \quad \lambda_{n,\perp} = b^n \prod_{i=1}^{n} x_i > 0. \tag{11}$$

The eigenvalue $\lambda_{n,\parallel}$ is the one well known from the logistic map $f(x)$, while the transverse eigenvalue $\lambda_{n,\perp}$ determines when the n-cycle on the x-axis is transversely attracting ($0 < \lambda_{n,\perp} < 1$) or repelling ($\lambda_{n,\perp} > 1$), and the bifurcation value is given by $\lambda_{n,\perp} = 1$ which corresponds to the condition

$$b = \frac{1}{\left(\prod_{i=1}^{n} x_i\right)^{1/n}}. \tag{12}$$

Another peculiarity occurs for an n-cycle with periodic points $\{(x_1, y_1), \ldots, (x_n, y_n)\}$ not belonging to the x-axis. From the definition of map T we have that it must satisfy $y_1 = b^n x_n \cdots x_1 y_1$ so that, being $y_1 \neq 0$, it must be $b^n \prod_{i=1}^{n} x_i = 1$. Thus, we have a relation between the product of the values x_i of the periodic points of the cycle and the parameter b, which corresponds to the same condition given in (12). It follows that if under parameter variation, a cycle of the x-axis undergoes a transverse bifurcation with eigenvalue which changes from $0 < \lambda_{n,\perp} < 1$ to $\lambda_{n,\perp} > 1$, since the bifurcation cannot be a fold one, then either it is a trancritical bifurcation or a pitchfork bifurcation (although we conjecture that it is a trancritical bifurcation).

Proposition 1. *Let $\lambda_{n,\perp} = b^n \prod_{i=1}^{n} x_i = 1$ for an n-cycle on the x-axis with periodic points $\{x_1, \ldots, x_n\}$, then it is merging with an n-cycle not belonging to the x-axis, which undergoes a trancritical bifurcation or a pitchfork bifurcation.*

2.1. *Stability of the fixed points*

For the origin O, it is $\lambda_{1,\parallel}(O) = a$ and $\lambda_{1,\perp}(O) = 0$ (related to the y-axis which is mapped into O), so that for $a > 1$, it is always a particular kind of saddle, whose stable set will be commented on below.

For the fixed point P_0, we have $\lambda_{1,\parallel}(P_0) = 2 - a$, $\lambda_{1,\perp}(P_0) = b(a - 1)$ and, as it is well known, it becomes unstable on the x-axis for $a > 3$ (the flip bifurcation at $a = 3$ leads to a 2-cycle on the x-axis) while it is transversely attracting for $b(a - 1) < 1$. Since $a > 1$, a bifurcation occurs with $\lambda_{1,\perp}(P_0) = 1$ at

$$b = \frac{1}{a - 1} \tag{13}$$

and at $b = \frac{1}{a-1}$, it is $x^* = \frac{1}{b} = a - 1$ and $y^* = a - 1 - \frac{1}{b} = 0$, leading to the merging of the two fixed points, $P_0 = P^*$, due to a transcritical bifurcation with respect to the transverse eigenvalue. In fact, for the fixed point P^* given in (4), we make use of the Jacobian matrix evaluated in P^*, with

$$\mathrm{Tr}(J^*) = 2 - \frac{1}{b}, \quad \mathrm{Det}(J^*) = a - \frac{2}{b} \tag{14}$$

and of the characteristic polynomial $\mathcal{P}(\lambda) = \lambda^2 - \mathrm{Tr}(J^*)\lambda + \mathrm{Det}(J^*)$, since it is well known that for the stability we can consider the three conditions $\mathcal{P}(1) = 1 - \mathrm{Tr}(J^*) + \mathrm{Det}(J^*) > 0$, $\mathcal{P}(-1) = 1 + \mathrm{Tr}(J^*) + \mathrm{Det}(J^*) > 0$, $\mathrm{Det}(J^*) < 1$, and explicitly

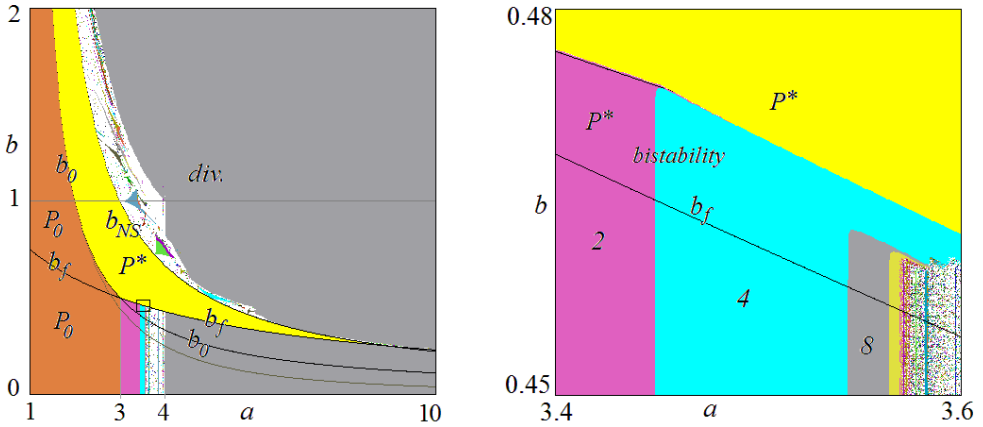

(a) (b)

Fig. 1. Two-dimensional bifurcation diagrams in the parameter plane (a, b). In (a) are evidenced the bifurcation curves related to $b = b_0$, $b = b_f$, $b = b_{\rm NS}$, and for $a > 3$ the curve $b = 4/a^2$ below which all the cycles existing on the x-axis are transversely attracting. Different colors represent attracting cycles of different periods. The gray points denote divergence. In orange (resp., yellow) the stability region of P_0 (resp., P^*). In (b) an enlargement of the rectangle shown in (a), where some periods are indicated, and the colored regions above the curve $b = b_f$ denote bistability, P^* is attracting as well as an attractor on the x-axis.

we have

$$\mathcal{P}(1) = a - 1 - \frac{1}{b} > 0 \quad \text{i.e. } b > b_0 := \frac{1}{a-1} \tag{15}$$

$$\mathcal{P}(-1) = 3 + a - \frac{3}{b} > 0 \quad \text{i.e. } b > b_f := \frac{3}{3+a} \tag{16}$$

$$\text{Det} = a - \frac{2}{b} < 1 \qquad \text{i.e. } b < b_{\rm NS} := \frac{2}{a-1}. \tag{17}$$

In the parameter plane (a, b), the three bifurcation curves occurring at $\mathcal{P}(1) = 0$, $\mathcal{P}(-1) = 0$ and Det $= 1$ related to the fixed point P^* are evidenced in Fig. 1. The curves $\mathcal{P}(1) = 0$ and $\mathcal{P}(-1) = 0$ (flip bifurcation of one eigenvalue) are intersecting at the point $(a, b) = (3, 0.5)$. The curves $\mathcal{P}(-1) = 0$ and Det $= 1$ are intersecting in $(a, b) = (9, 0.25)$. The bifurcation occurring at $\mathcal{P}(1) = 0$ corresponds to the merging of the fixed point P^* with P_0 already commented above, the fixed point P^* is below the x-axis for $\mathcal{P}(1) < 0$ while it is above the x-axis for $\mathcal{P}(1) > 0$, and it corresponds to a transcritical bifurcation related to the transverse eigenvalue, which has different dynamic behaviors depending on $a < 3$ or $3 < a < 9$.

The bifurcation occurring at Det $= 1$ is a Neimark–Sacker bifurcation, while in the next subsection, we shall prove that the flip bifurcation occurring at $P(-1) = 0$ is of subcritical type and associated with a 2-cycle not belonging to the x-axis, whose periodic points are explicitly given.

2.1.1. *2-cycles and related stability*

Besides the 2-cycle on the invariant x-axis, map T can have a 2-cycle not belonging to the invariant line. The one on the x-axis is related to the flip bifurcation of P_0 with the eigenvalue $\lambda_{1,\|}(P_0) = 2 - a$, occurring at $a = 3$, and it is given (for $a > 3$) by $\{(\xi_-, 0), (\xi_+, 0)\}$ where

$$\xi_\pm = \frac{1}{2}(a + 1 \pm \sqrt{(a+1)(a-3)}). \tag{18}$$

As it is well known from the logistic map, this 2-cycle on the x-axis is attracting on the invariant line as long as it is $\lambda_{2,\|} > -1$. From (11) we have

$$\begin{aligned} \lambda_{2,\|} &= (a - 2\xi_-)(a - 2\xi_+) = -a^2 + 2a + 4, \\ \lambda_{2,\perp} &= b^2 \xi_- \xi_+ = b^2(1 + a) \end{aligned} \tag{19}$$

so that the bifurcation related to $\lambda_{2,\|} = -1$ occurs for $a^2 + 2a + 4 = -1$ leading to $a = 1 + \sqrt{6} \approx 3.449489743$. The transverse eigenvalue is $\lambda_{2,\perp} = b^2 \xi_- \xi_+$, and a bifurcation for $\lambda_{2,\perp} = 1$ leading to $b = \frac{1}{\sqrt{1+a}}$.

A second 2-cycle $\mathcal{C}_2$ may exist, external to the x-axis. In fact, considering the solutions of

$T^2(x,y)=(x,y)$ we obtain the system

$$\begin{cases} x = x(a-x-y)[a-x(a-x-y)-bxy] \\ y = b^2x^2y(a-x-y) \end{cases} \tag{20}$$

that is

$$\begin{cases} 1 = (a-x-y)[a-x(a-x-y)-bxy] \\ 1 = b^2x^2(a-x-y), \end{cases}$$

from the second equation we have

$$y = -\frac{1}{b^2x^2} + a - x \tag{21}$$

and from the first equation:

$$b(1-b)x^3 - bax^2 + ax - \frac{1-b}{b^2} = 0.$$

Since a solution is the fixed point P^* we can factorize as

$$\left(x - \frac{1}{b}\right)(\alpha x^2 + \beta x + \gamma) = 0 \tag{22}$$

where

$$\alpha = b(1-b), \quad \beta = (1-b-ab), \quad \gamma = \frac{1-b}{b} \tag{23}$$

so that the solutions $(x_\pm, y_\pm)$ exist for $b \neq 1$ and

$$(\beta^2 - 4\alpha\gamma) = (3-3b-ab)(b-ab-1) > 0 \tag{24}$$

which corresponds to $b > \frac{3}{3+a}$, i.e. $b > b_f$, and it is

$$x_\pm = \frac{ab+b-1 \pm \sqrt{(3-3b-ab)(b-ab-1)}}{2b(1-b)} \tag{25}$$

while the values $y_\pm$ come from (21). Notice that this also proves that for $b=1$ the 2-cycle $\mathcal{C}_2$ does not exist.

It is easy to see that for $b=b_f$, the two periodic points are merging with P^*, that is $(x_\pm, y_\pm) = (x^*, y^*) = (\frac{1}{b}, a-1-\frac{1}{b})$.

The 2-cycle $\mathcal{C}_2$ so determined, whose appearance is related to the flip bifurcation of the fixed point P^*, also evidences that increasing b the 2-cycle exists after the flip bifurcation related to one eigenvalue of P^* for $b > b_f$, which means that for $a < 3$ this transition leads from P^* repelling node in the region $y < 0$, to saddle and the internal 2-cycle saddle $\mathcal{C}_2$ appears in the region $y < 0$, while for $a > 3$ this transition leads from P^* saddle in the region $y > 0$ to P^* attracting node, and the 2-cycle saddle $\mathcal{C}_2$ appears in the region $y > 0$.

The 2-cycle $\mathcal{C}_2$ is also related to the transcritical bifurcation of the 2-cycle on the x-axis, occurring, as detected above, for $\lambda_{2,\perp} = 1$. In fact, when the parameters satisfy $b^2(1+a) = 1$, from (23) we have

$$\alpha = b(1-b), \quad \beta = -\frac{1-b}{b}, \quad \gamma = \frac{1-b}{b}$$

so that $x_\pm$ are the roots of the equation

$$b^2x^2 - x + 1 = 0 \tag{26}$$

and from (21) we have that $y = -\frac{1}{b^2x^2} + a - x = 0$ holds when $x_\pm$ are the roots of the same equation in (26). Thus, when $\lambda_{2,\perp} = 1$ holds then the 2-cycle $\mathcal{C}_2$ merges with the 2-cycle on the x-axis. Note that fixing the value of the parameter a and increasing b, we have that $b_f = \frac{3}{3+a} < \frac{1}{\sqrt{1+a}}$ holds for $a > 3$. We have so proved the following:

Proposition 2. *At $b = b_f$ ($b_f = \frac{3}{3+a}$) the fixed point P^* undergoes a subcritical flip bifurcation associated with the 2-cycle $\mathcal{C}_2$, whose periodic points $(x_\pm, y_\pm)$ exist for $b > b_f$ and are given by*

$$x_\pm = \frac{ab+b-1 \pm \sqrt{(3-3b-ab)(b-ab-1)}}{2b(1-b)}, \tag{27}$$

$$y_\pm = -\frac{1}{b^2{x_\pm}^2} + a - x_\pm. \tag{28}$$

For $3 < a < 9$ the 2-cycle $\mathcal{C}_2$ is a saddle at its appearance, and undergoes a transcritical bifurcation with the 2-cycle on the x-axis at $b = \frac{1}{\sqrt{1+a}}$ (from the region $y > 0$ to the region $y < 0$, increasing b). For $b = 1$ and $a > 1$ the 2-cycle $\mathcal{C}_2$ cannot exist.

2.2. *Stable set of O and boundary of B(∞)*

It is known that for the logistic map on the x-axis the origin O and it preimage O^{-1} ($x = a$) belong to the boundary of the set of divergent trajectories denoted by $B(\infty)$. For map T the y-axis is mapped into the origin O so that it belongs to its stable set. That is, this fixed point is not a regular saddle with a branch of stable set having points with trajectories convergent to the fixed point. Any point $(0,y)$ is mapped into O in one iteration, and the stable

set of O consists of all the preimages of any rank of the point itself: $W^S(O) = U_{n=0}^{\infty} T^{-n}(0,0)$. Since O belongs to the border of $B(\infty)$, it follows also that all its preimages of any rank satisfy the same property, starting from the y-axis which is $T^{-1}(0,0)$, and related preimages due to the points of the half-line of the y-axis below LC, which we denote by ω^0, that is, the half-line on $x = 0$ belonging to the region Z_2, for $y \le b\frac{a^2}{4}$. We have the following:

Proposition 3. *The stable set* $W^S(O) = \{x = 0\} \cup U_{n=1}^{\infty} T^{-n}(\omega^0)$ *belongs to the boundary* $\partial B(\infty)$.

It is worth to investigate in more detail the structure of $W^S(O)$, to be used in the next sections. From (6) the two inverses of a point $(0, t)$ of ω^0 are given by

$$\omega^{-1}: \quad x = \frac{a}{2} \pm \frac{1}{2}\sqrt{a^2 - 4\frac{t}{b}}, \qquad y = \frac{t}{bx}; \quad y = a - x \tag{29}$$

and eliminating the parameter t from these equations, we have that the points belong to the line of equation $y = a - x$, on which the two half-lines $\omega_{1,2}^{-1}$ are separated from the point $(\frac{a}{2}, \frac{a}{2})$.

To have a further preimage, let us consider a point $(t, a - t)$ belonging to Z_2 and we take the preimages from (6) obtaining the parametric equations

$$\omega^{-2}: \quad x = \frac{a}{2} \pm \frac{1}{2}\sqrt{a^2 - 4\left(t + \frac{a-t}{b}\right)}, \qquad y = \frac{a-t}{bx} \tag{30}$$

from which, eliminating the parameter t, we get the following Cartesian equation for $b \neq 1$:

$$\omega^{-2}: \quad y = \frac{a - (a-x)x}{x(b-1)} \tag{31}$$

while for $b = 1$ the preimages ω^{-2} are two half-lines at $x = \frac{a}{2} \pm \frac{1}{2}\sqrt{a^2 - 4a}$.

Besides the stable set of the origin, let us take note that the unstable branch of the origin in the region $x < 0$ has divergent trajectories for any $a > 1$, the unstable branch for $x > 0$ is the interval $[0, c]$ for $a \le 4$, where c denotes the critical point of $f(x)$. Such points are also related to the intersection of the critical lines LC_i with the x-axis, let us denote $c_{-1} = \frac{a}{2}$ and $c = f(c_{-1}) = \frac{a^2}{4}$. For $a > 4$ also the unstable branch for $x > 0$ has almost all the points with divergent trajectories (since it is $c = \frac{a^2}{4} > a$), although the origin always belongs to a Cantor set of zero measure bounded in $[0, a]$.

2.3. *Attracting sets of map T on the x-axis*

As we can argue from the transverse eigenvalue of the cycles belonging to the x-axis, it is possible that all of them are transversely attracting, in which case the attracting sets on the x-axis are topological or Milnor attractors for map T, as unique attracting set or coexisting with some other attracting set of T.

The bifurcations occurring on the invariant set on the x-axis related to the logistic map $f(x)$ are well known (see [Mira, 1987; Devaney, 1989; Mira *et al.*, 1996]), and increasing a, for $a > 3$, we have attracting cycles of period 2^n up to the first Feigenbaum point, after which the attracting set (a cycle or invariant cyclical chaotic intervals or a critical set [Jacobson, 1981; Mira, 1987; Sharkovsky *et al.*, 1997; Thunberg, 2001]) is always located in the interval $[c_1, c]$ bounded by the critical points c and c_1 of $f(x)$, where $c_1 = f(c) = \frac{a^2}{4}(a - \frac{a^2}{4})$.

It is also well known that any attracting cycle is attracting (for the logistic) for an open interval of values of a, and that the set of values of a at which we have chaotic intervals is of positive Lebesgue measure [Jacobson, 1981; Thunberg, 2001]. For $a > 4$ the bounded invariant set is a Cantor set of points in $[0, a]$ with chaotic dynamics, and of zero measure.

Since for any cycle different from O it is $\lambda_{n,\perp} = b^n \prod_{i=1}^{n} x_i > 0$ and any periodic point satisfies $0 < x_i < c = \frac{a^2}{4}$ we have $0 < \lambda_{n,\perp} < (b\frac{a^2}{4})^n$ so that a sufficient condition to have $\lambda_{n,\perp} < 1$ for any cycle is $b\frac{a^2}{4} < 1$. We have so proved the following:

Proposition 4

(i) *Let* $0 < b < 0.25$, *then for any* $a \in [1, 4]$ *all the cycles existing on the x-axis are transversely attracting.*

(ii) *Let* $a > 1$, *then for* $b < 4/a^2$ *all the cycles existing on the x-axis are transversely attracting.*

(iii) *Any n-cycle on the x-axis different from O with periodic points* $\{x_1, \ldots, x_n\}$ *is transversely attracting for* $b < 1/(\prod_{i=1}^{n} x_i)^{1/n}$.

From Proposition 4 we have that whenever an attracting cycle of the logistic map exists (which occurs for an open interval of values for a), then it is also a topological attractor for map T at low values of the parameter b, and the condition given in the proposition is only a sufficient condition to have all the cycles transversely attracting. For any single cycle the transversality condition changes at any fixed value of a and increasing b (since fixing a the periodic points do not change). As we have seen above, the 2-cycle given in (18), which exists as attracting in a given interval $[a_-, a_+]$, becomes transversely repelling at $b = 1/\sqrt{1+a}$.

Clearly, if in the region $y > 0$ or $y < 0$ some different attracting set exists, then we have coexistence, at least bistability. In effect, in general, the attracting sets not belonging to the x-axis are located in the triangle Δ in the region $y > 0$, bounded by the segments $[0, a]$ on the axes of the phase plane (x, y) and the diagonal connecting $(0, a) - (a, 0)$, which is a portion of the preimage ω^{-1}, but not always. It is very interesting for this class of maps to determine attracting cycles or attracting chaotic sets also in the region $y < 0$, as we shall see in the following sections.

The property of positive transversal eigenvalues for cycles belonging to the x-axis also leads to the fact that the x-axis is an invariant set which separates regions having often, when the x-axis is not attracting, different dynamic behaviors. This is due to the fact that points close to the invariant set on opposite sides are repelled in different directions, above and below it. In particular, it is interesting the already mentioned triangle Δ, which has been considered in the literature related to this map for $b = 1$ and $a > 1$, since it may include the fixed point P^* in its interior. Also in our more general case $b > 0$ this region plays an important role, especially when it is mapped into itself. We prove the following:

Proposition 5. *Let* $1 < a < 4$ *and* $0 < b < 4/a$, *then* $T(\Delta) \subset \Delta$ (*strictly*).

Proof. As it is immediate to see, a point $(x, y) \in \Delta$ has $(x', y') = T(x, y)$ belonging to the first quadrant of the plane. The assumptions on the parameters a and b are such that the segment of LC in the first quadrant is inside Δ and LC is below the diagonal of Δ, segment of ω^{-1}, so that all the points of the positive quadrant above this arc of LC belong to the region Z_0, which means that no point can be mapped there. In particular, no point can be mapped in the region between this arc of LC and the diagonal of Δ, so that $T(\Delta)$ is strictly mapped into itself. ■

Clearly, this triangle Δ mapped into itself is candidate to host attracting and repelling sets, and although it cannot attract points from the invariant x-axis, it may attract points from the region $y < 0$.

2.4. *Bifurcation sequences for* $1 < a < 3$ *as a function of* b

As determined above, the bifurcation sequences increasing the transverse parameter b at each fixed value of the parameter a is different for $a < 3$ (when P_0 is attracting on the x-axis) and $3 < a < 9$ (when P_0 is repelling on the x-axis). For $1 < a < 3$ and increasing b from 0, the fixed point P^* is a repelling node in the region $y < 0$ and belongs, with all its preimages, to the boundary $\partial B(P_0)$ as well as to $\partial B(\infty)$. Increasing b first the bifurcation $\mathcal{P}(-1) = 0$ (at $b = b_f$) occurs, leading to a 2-cycle saddle in the region $y < 0$, and then the bifurcation $\mathcal{P}(1) = 0$ (at $b = b_0$) after which P_0 becomes a saddle transversely repelling and P^* an attracting node in the region $y > 0$.

An example is shown in Fig. 2 at $a = 2.7$ and fixed and increasing $b > 0$. In Fig. 2(a) at $b = 0.52$ the fixed point P_0 is an attracting node for map T, and we have evidenced its basin of attraction in red (separating the set of points having divergent trajectories), and the boundary, besides the stable set of the origin, includes the repelling node P^* and all its preimages. At $b = b_f \approx 0.5363$ the fixed point P^* becomes a saddle and the saddle 2-cycle $\mathcal{C}_2$ also belongs to $\partial B(\infty)$.

Increasing b, the saddle 2-cycle $\mathcal{C}_2$ undergoes a subcritical flip bifurcation, becoming an attracting node, and leaving a saddle 4-cycle on the boundary $\partial B(\infty)$. Thus we have coexistence of two topological attractors, besides P_0 on the x-axis there is the 2-cycle $\mathcal{C}_2$ attracting node in the region $y < 0$ [shown in Fig. 2(b)]. Increasing b the 2-cycle $\mathcal{C}_2$ becomes unstable and belongs to the boundary $\partial B(\infty)$ [see Fig. 3(a)] before the bifurcation of the two fixed points, when P^* and P_0 are merging, occurring at $b = b_0 \approx 0.588$, leaving P^* attracting node and unique attractor. The simulations [see Fig. 3(b)] show that its basin of attraction is the triangle Δ. Increasing b the fixed point P^* undergoes a NS bifurcation at $b = b_{\rm NS}$.

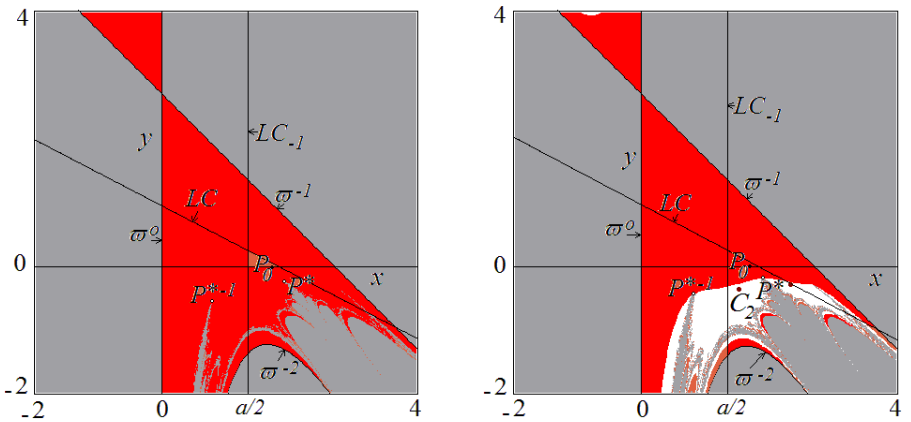

Fig. 2. Phase plane at $a = 2.7$. In (a) $b = 0.52$, P_0 is attracting, its basin of attraction is in red, and on the boundary the repelling node P^* and its preimage $P^{*,-1}$ are observed. In (b) $b = 0.53$, P_0 is attracting, its basin of attraction is in red, coexisting with the 2-cycle C_2 attracting node, whose basin is in white. The gray points denote divergence.

2.5. *Transitions for $3 < a < a_\infty$*

Differently, for $3 < a < 9$ and increasing b first the merging bifurcation $\mathcal{P}(1) = 0$ (at $b = b_0$) occurs, leading P_0 from saddle to repelling node, and the repelling node P^* from $y < 0$ to a saddle in the region $y > 0$. This means that the attracting set existing for the logistic map $f(x)$ on the x-axis, for $a < 4$, persists as a topological attractor for map T also after the bifurcation at $b = b_0$. But clearly, by increasing b several bifurcations may occur in the region $y > 0$, and not only, since also in the region $y < 0$ bifurcations can take place.

As a typical example in the range before the first Feigenbaum point $a_\infty \approx 3.56994567$ in which the attracting set for the logistic map is a 2^n-cycle, let us consider the case at $a = 3.55$. At this value, on the x-axis the fixed point P_0, the 2-cycle and the 4-cycle are unstable in the parallel direction, and saddle of map T at low values of b, while an attracting 8-cycle exists, which is the only attractor also for map T. When P^* and P_0 are merging, occurring at $b = b_0 \approx 0.392156$, as well as soon after the bifurcation, the only attracting set of map T is the 8-cycle on the x-axis, up to the subcritical flip bifurcation of P^* which takes place at $b = b_f \approx 0.458$ leading to P^* attracting, so that map T has two coexisting topological attractors. The 2-cycle saddle $\mathcal{C}_2$ belongs to the border of the basins of P^* and of the attracting 8-cycle on the x-axis. An example is shown in Fig. 4(a). Increasing b,

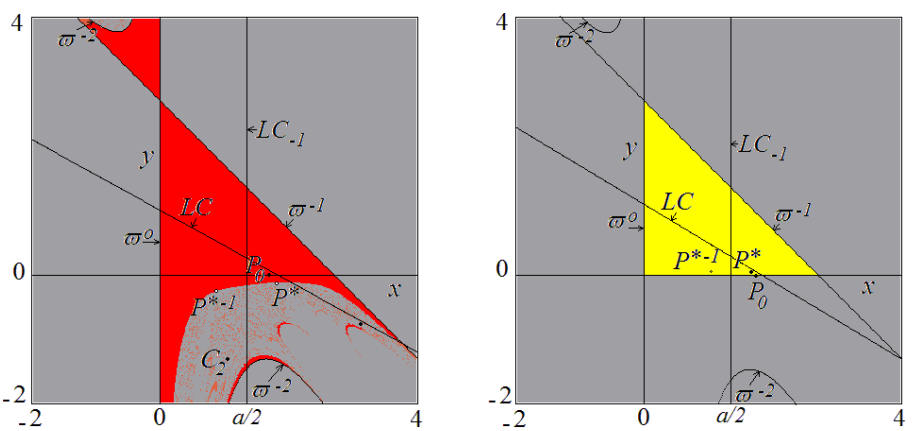

Fig. 3. Phase plane at $a = 2.7$. In (a) $b = 0.55$, P_0 is attracting, its basin of attraction is in red, and on the boundary the saddle P^*, its preimage $P^{*,-1}$, and the unstable 2-cycle C_2 are observed. In (b) $b = 0.6$, P^* is the only attractor internal to Δ, in yellow is its basin of attraction. The gray points denote divergence.

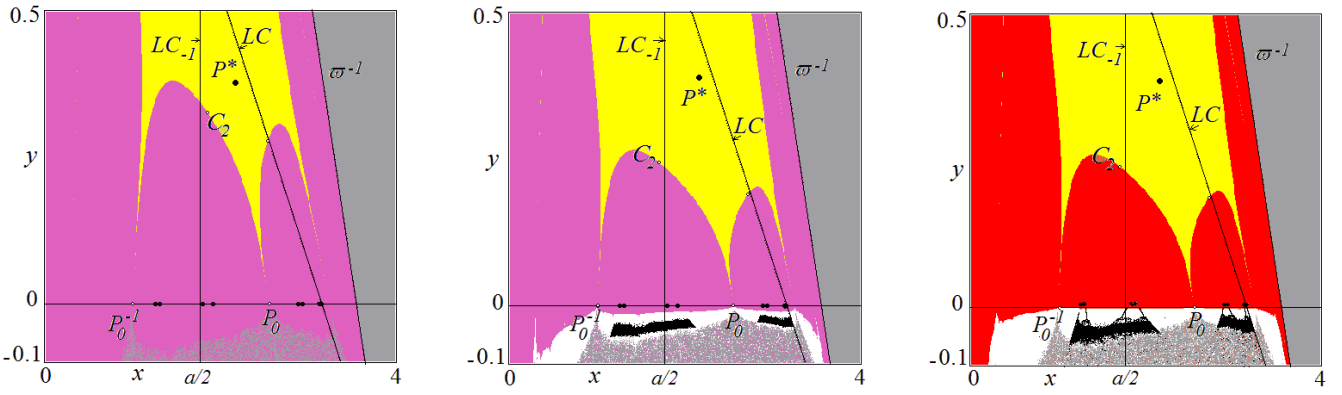

Fig. 4. Phase plane at $a = 3.55$. In (a) $b = 0.46$, P^* is the only attractor internal to Δ, its basin of attraction is in yellow, in pink is the basin of attraction of the attracting 8-cycle on the x-axis. In (b) $b = 0.4625$, besides the two attractors as in (a) one more chaotic attractor exists in the region $y < 0$, in white is its basin of attraction. In (c) $b = 0.4626$, P^* is attracting and coexists with an attracting 8-cycle internal to Δ, the 8-cycle on the x-axis is transversely repelling, here the white points have a chaotic transient and then diverge. The gray points denote divergence.

when the 8-cycle is still attracting for T, but close to the transverse bifurcation, one more attracting set for T appears in the region $y < 0$, with chaotic dynamics, as shown in Fig. 4(b) and we conjecture that an 8-cycle saddle from the region $y < 0$ on the frontier below the x-axis is merging with the attracting 8-cycle on the x-axis at the transverse bifurcation, when $\lambda_{8,\perp} = b^8 \prod_{i=1}^{8} x_i = 1$. After the transcritical bifurcation, an 8-cycle attracting node exists above the x-axis, it is numerically observable, as shown in Fig. 4(c), while the 8-cycle on the x-axis becomes transversely repelling, a saddle for T. Thus, two different topological attractors exist in the region $y > 0$, while in the region $y < 0$ related to the former attracting set, we detected transient chaotic dynamics before ending in divergent trajectories.

3. Milnor Attractors, Riddled Basins and Blowout Bifurcations

As mentioned in the Introduction, we are interested in the bifurcations occurring in the transverse direction, when the attracting set $\mathcal{A}$ on the x-axis, for the logistic map $f(x)$, consists of chaotic intervals. We know that for each value of a only one attracting set exists for $f(x)$ on the x-axis. In particular, after the first Feigenbaum point there are homoclinic bifurcations of cycles of even periods leading to cyclic chaotic intervals. As an example, we consider those related to the merging of 2^{n+1} absorbing intervals into 2^n chaotic intervals, bounded by the first 2^{n+1} images of the critical point $c_{-1} = a/2$, $f^i(c_{-1})$ for $i = 1, \ldots, 2^{n+1}$, and first homoclinic bifurcation of the 2^n cycle internal to the 2^n chaotic intervals, occurring at particular bifurcation values for a.

We shall consider the merging of eight absorbing intervals into four chaotic intervals A at the first homoclinic bifurcation of the 4-cycle with symbolic sequence $(\mathrm{LR})^2$, occurring approximately at $a = 3.574805$, the merging of four absorbing intervals into two chaotic intervals $\mathcal{A} = [c_1, c_3] \cup [c_2, c]$ at the first homoclinic bifurcation of the 2-cycle at $a = 3.592572184$, and the merging of two absorbing intervals into one chaotic interval $\mathcal{A} = [c_1, c]$ at the first homoclinic bifurcation of the fixed point P_0 at $a = 3.67857351$.

Recall that b is a normal parameter, it influences only the transverse eigenvalue of a point of the x-axis. In all the three cases mentioned above $\mathcal{A}$ is a chaotic attractor for the logistic map, and from Proposition 4 at low values of b, it is also a topological attractor of map T, since all the saddle cycles existing in the chaotic intervals are transversely attracting [that is, $\Lambda_{\perp}^{\max}$ in (3) is negative]. Clearly, as soon as one of the cycles existing in $\mathcal{A}$ becomes transversely repelling, $\mathcal{A}$ becomes a Milnor attractor with a stable set which may be riddled into some other basin of attraction. This stable set has a positive Lebesgue measure but it does not include any open neighborhood. In our case, the natural transverse Lyapunov exponent [from (2)] related to the aperiodic orbit $\{x_i = f^i(x_0), i \geq 0\}$ of a point

x_0 for map $f(x)$ is given by

$$\Lambda_{\perp}^{\text{nat}} = \lim_{N\to\infty} \frac{1}{N} \sum_{i=0}^{N} \ln|bx_i|$$

$$= \ln(b) + \lim_{N\to\infty} \frac{1}{N} \sum_{i=0}^{N} \ln(x_i) \qquad (32)$$

which can be numerically computed. Thus, as long as it is $\Lambda_{\perp}^{\text{nat}} < 0$ (which means that on average are dominating the cycles in the chaotic intervals which are transversely attracting) the chaotic attractor $\mathcal{A}$ of $f(x)$ leads to a Milnor attractor for T, since there exists a stable set of positive measure. We know that the increase of b leads to more and more cycles transversally repelling. Thus, as b increases the stable set of $\mathcal{A}$ has a positive Lebesgue measure which decreases and $\Lambda_{\perp}^{\text{nat}}$ increases, approaching 0. The blowout bifurcation occurs when the transverse Lyapunov exponent $\Lambda_{\perp}^{\text{nat}}$ becomes positive, which means that the transversely repelling cycles are dominating and the stable set of $\mathcal{A}$ becomes of zero Lebesgue measure.

In all the cases mentioned above, it is interesting to describe the effect of the riddling bifurcations (transition from a topological attractor to a Milnor attractor), and in particular the blowout bifurcations, since these are global bifurcations whose results depend on the global behaviors of the map.

3.1. *Transitions with four chaotic intervals at* $a = 3.574805$

Let us consider $a = 3.574805$ at which the logistic map $f(x)$ on the x-axis has four cyclic chaotic intervals $\mathcal{A}$, at the first homoclinic bifurcation of the 4-cycle $(\text{LR})^2$ for which the product of the four periodic points is $\prod_{i=1}^{4} x_i = 22.4146$. It follows that the 4-cycle is transversely attracting as long as the condition $\lambda_{4,\perp} = b^4 \prod_{i=1}^{4} x_i < 1$ holds, that is, $b < 0.459586$. The fixed point P^* becomes attracting at $b = b_f = 0.456287$, and for $0 < b < b_f$ the only attracting set observed numerically is the chaotic set $\mathcal{A}$ on the x-axis, and it is possible that all the cycles belonging to the four chaotic intervals are transversely attracting, an example is shown in Fig. 5(a) at $b = 0.45$. For $b_f < b < 0.459586$ the internal fixed point P^* is attracting and the four chaotic intervals on the x-axis are also attracting a set of points with positive measure, since it seems $\Lambda_{\perp}^{\max} = \ln(\lambda_{4,\perp})$. So, after the transverse bifurcation of the 4-cycle (corresponding to the riddling bifurcation), for $b > 0.459586$ we have that P^* is a topological attractor while $\mathcal{A}$ is a Milnor attractor with a stable set riddled into $B(P^*)$. An example is shown in Fig. 5(b) at $b = 0.4601$.

Computing the transverse Lyapunov exponent of a chaotic trajectory on the x-axis we have $\Lambda_{\perp}^{\text{nat}} < 0$ at $b = 0.4601$, while it is $\Lambda_{\perp}^{\text{nat}} > 0$ at $b = 0.4602$. Thus, between these two values, we have the blowout bifurcation. We show in Fig. 6 at $b = 0.4602$ that the invariant set on the x-axis is no longer a Milnor attractor (it has a stable set of zero measure), and the effect of the global bifurcation in this case is the appearance of two more topological attractors, coexisting with the attracting fixed point P^*, two distinct 4-pieces chaotic attracting sets, one in the region $y < 0$ and one in the region $y > 0$, as clearly shown in the enlargement of Fig. 6(b).

The two new topological attractors persist for an interval of values of b, increasing in size, and farther from the x-axis. Moreover, increasing b an attracting cycle of period 24 appears via saddle-node bifurcation in the region $y > 0$, leading to four coexisting topological attractors, as shown in Fig. 7 at $b = 0.4603$.

3.2. *Transitions with two chaotic intervals at* $a = 3.592572184$

A different dynamic behavior occurs when we consider $a = 3.592572184$ (at which for the logistic map $f(x)$ the chaotic attractor $\mathcal{A}$ consists of two cyclical intervals). Increasing b, the fixed point P^* enters the region $y > 0$ at $b = b_0 = 0.38571732$ and becomes attracting at the subcritical flip bifurcation, at $b = b_f = 0.455057588$. The two chaotic intervals now include a 2-cycle and a 4-cycle, and the 4-cycle is the one which first becomes transversely repelling, the product of the periodic points gives $\prod_{i=1}^{4} x_i = 22.81058478$, from which it follows that the transversal direction is attracting as long as $b < 0.4575788$. While the 2-cycle on the x-axis has the product of the periodic points given by $\prod_{i=1}^{2} x_i = 4.592572184$, and it is transversely attracting as long as $b < 0.466629299$ (this transverse bifurcation is also the bifurcation at which the 2-cycle $\mathcal{C}_2$ merges with the 2-cycle on the x-axis).

It follows that for $0 < b < b_f$ the only attracting set is $\mathcal{A}$ on the x-axis while for $b_f < b < 0.4575788$ the fixed point P^* is also attracting, so that we have two coexisting attractors, an example is shown in Fig. 8(a).

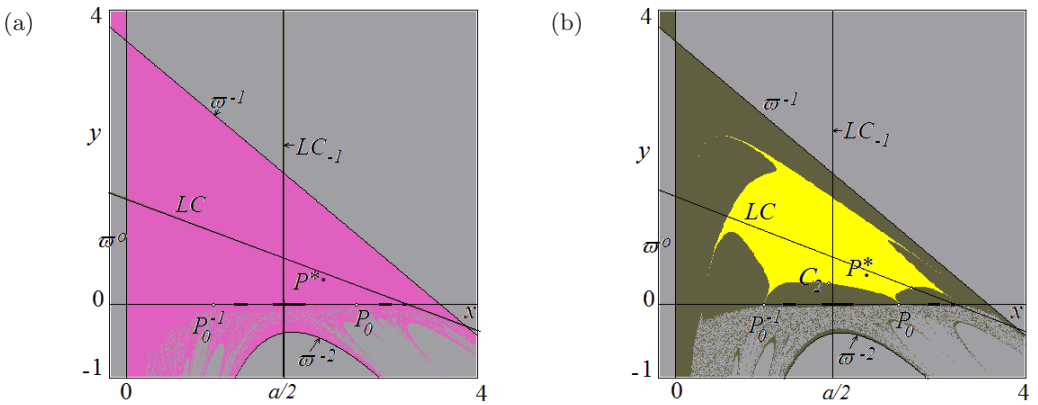

Fig. 5. Phase plane at $a = 3.574805$, on the x-axis, the four cyclic chaotic intervals $\mathcal{A}$ are attracting for map $f(x)$. In (a) $b = 0.45, \mathcal{A}$ is the only attractor, in pink is its basin of attraction. In (b) $b = 0.4601, P^*$ is attracting (its basin is in yellow) and coexisting with the Milnor attractor on the x-axis, the four cyclic chaotic intervals $\mathcal{A}$ (its stable set is in dark green). The gray points denote divergence.

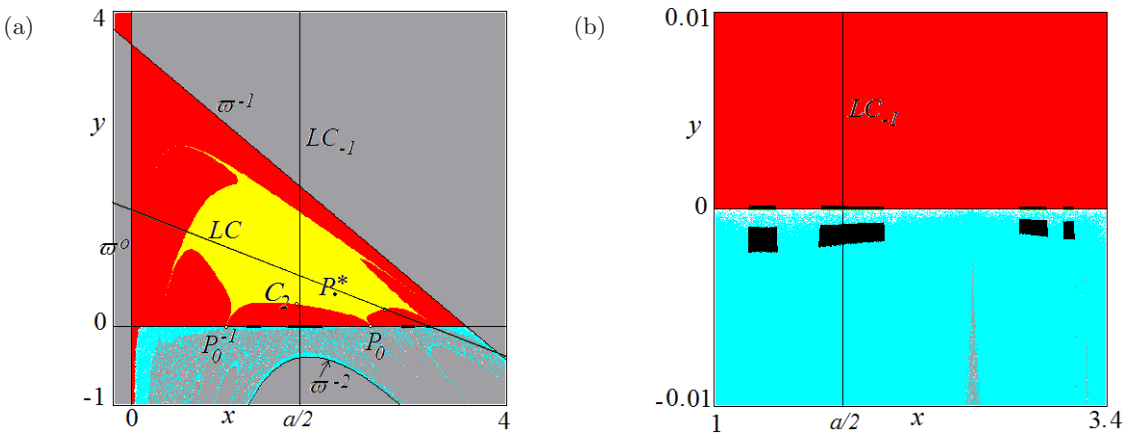

Fig. 6. Phase plane at $a = 3.574805, b = 0.4602$, on the x-axis, the four cyclic chaotic intervals $\mathcal{A}$ are attracting for map $f(x)$, but after the blowout bifurcation its stable set for map T is of zero measure. In (a) there are three topological attractors, P^*, with basin in yellow, and two 4-cyclical chaotic sets on opposite sides of the x-axis, evidenced in the enlargement in (b) and basins of different colors.

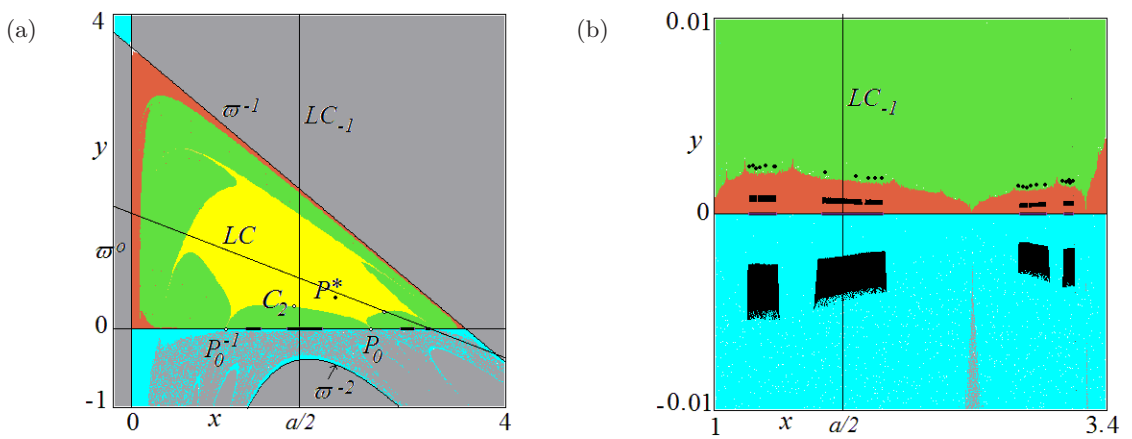

Fig. 7. Phase plane at $a = 3.574805, b = 0.4603$, on the x-axis, the four cyclic chaotic intervals $\mathcal{A}$ are attracting for map $f(x)$, but its stable set for map T is of zero measure. In (a) there are four topological attractors, besides the three shown in Fig. 6, there is an attracting cycle of period 24 whose basin is shown in green, the two cyclical chaotic sets on opposite sides of the x-axis, and the 24-cycle, are evidenced in the enlargement in (b) with basins of different colors.

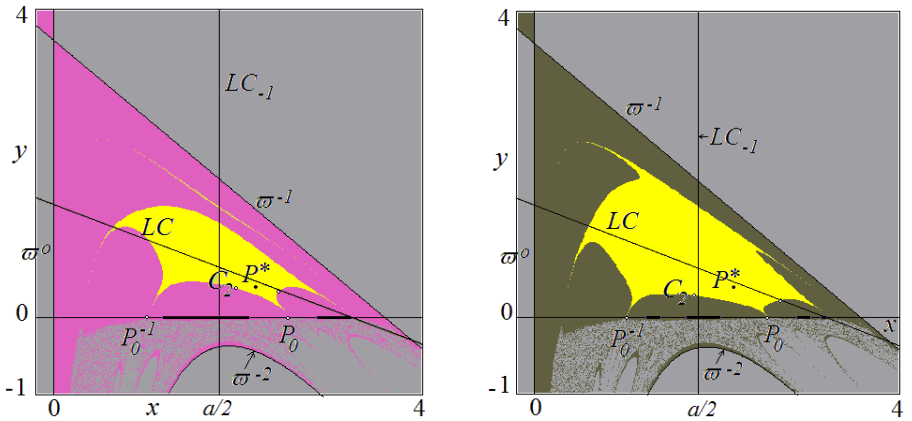

Fig. 8. Phase plane at $a = 3.592572184$, on the x-axis, the two cyclic chaotic intervals $\mathcal{A}$ are attracting for map $f(x)$. In (a) $b = 0.456$, P^* is attracting (its basin is in yellow) and coexisting with the attractor $\mathcal{A}$, whose basin is in pink. In (b) $b = 0.458$, P^* is attracting in the yellow basin, and coexisting with the Milnor attractor on the x-axis, the two cyclic chaotic intervals $\mathcal{A}$ (its stable set is in dark green). The gray points denote divergence.

The 4-cycle is responsible for the riddling bifurcation, and for $b > 0.4575788$ the 4-cycle on the x-axis (internal to the chaotic intervals) is transversely repelling, so that $\mathcal{A}$ becomes a Milnor attractor, an example is shown in Fig. 8(b) at $b = 0.458$. Increasing b, besides the fixed point P^* and the Milnor attractor $\mathcal{A}$ of two chaotic intervals on the x-axis, we observe the appearance of one more topological attractor consisting of four chaotic pieces numerically observed close to the x-axis in the region $y > 0$ (before the blowout bifurcation), an example is shown in Fig. 9(a) at $b = 0.4589$, where the enlargement in Fig. 9(b) shows the new chaotic topological attractor. Clearly, increasing b the stable set of the Milnor attractor on the x-axis decreases, an example at $b = 0.4609$ is shown in Fig. 9(c), where the attracting set with basin in red, coexisting with P^*, is now a 4-cycle (obtained from the chaotic pieces via a sequence of reverse bifurcations).

Computing the natural transverse Lyapunov exponent on the x-axis we have $\Lambda_{\perp}^{\text{nat}} < 0$ at $b = 0.4609$ [Fig. 9(c)], while it is $\Lambda_{\perp}^{\text{nat}} > 0$ at $b = 0.461$ so that the blowout bifurcation occurs in this interval, after which only the two topological attractors shown in Fig. 9(c) are left, and the stable set of $\mathcal{A}$ becomes of zero measure. In our numerical computations the blowout bifurcation now does not lead

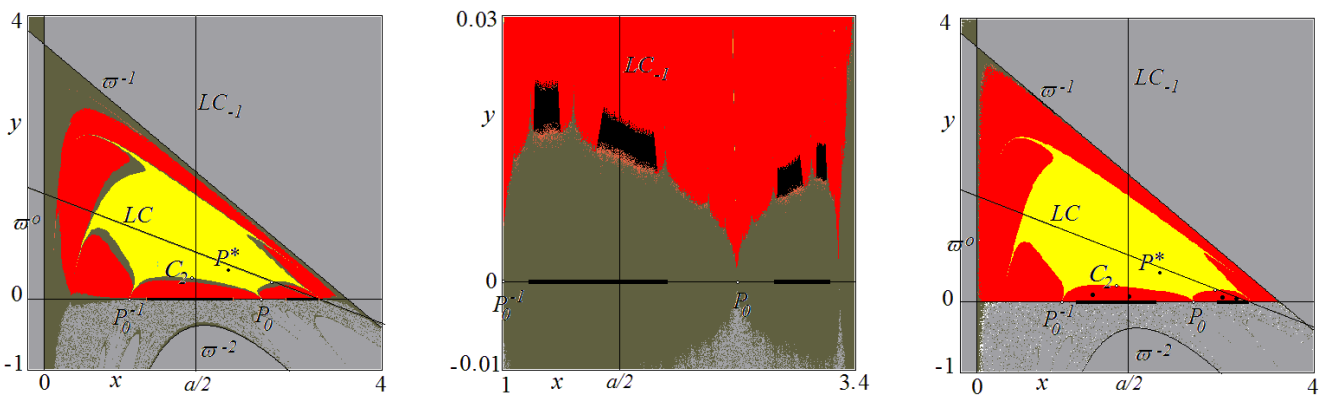

Fig. 9. Phase plane at $a = 3.592572184$, on the x-axis, the two cyclic chaotic intervals $\mathcal{A}$ are attracting for map $f(x)$. In (a) $b = 0.4589$, two topological attractors exist, P^*, whose basin is in yellow, and a 4-cyclical chaotic set whose basin is in red, and the Milnor attractor on the x-axis whose basin is in dark green, as evidenced in the enlargement in (b). In (c) $b = 0.4609$, close to the blowout bifurcation the stable set of the Milnor attractor (in dark green) is reduced, but still of positive measure, and the attracting set with basin in red is now a 4-cycle.

to an attracting set in the region $y < 0$, where the generic trajectory is divergent.

3.3. *Transitions with one chaotic interval at* $a = 3.67857351$

The fixed point P_0 (which is in the interior to the chaotic interval $\mathcal{A} = [c_1, c]$) becomes transversely repelling when the fixed point P^* enters (as a saddle) the region $y > 0$ at $b = b_0 = 0.373333$, and this is also the riddling bifurcation of $\mathcal{A}$, from topological attractor (for $0 < b < b_0$) to Milnor attractor. However, for $b > b_0$ close to the bifurcation there is no other attracting set numerically observable, thus the stable set of $\mathcal{A}$ is a set not riddled in some other basin of attraction, and its closure is a whole area, an example is shown in Fig. 10(a).

The peculiarity of this case is that between the riddling bifurcation and the blowout bifurcation there is only the Milnor attractor $\mathcal{A}$. In fact, the fixed point P^* becomes attracting at $b = b_f = 0.44919772$ and computing $\Lambda_\perp^{\text{nat}}$ on the x-axis, we have $\Lambda_\perp^{\text{nat}} < 0$ at $b = 0.426$, while it is $\Lambda_\perp^{\text{nat}} > 0$ at $b = 0.428$. Thus, the blowout bifurcation occurs at a value b_{blow} in the interval $(0.426, 0.428)$ when P^* is still a saddle. It follows that for $b_0 < b < b_{\text{blow}}$ map T has no topological attractor, but only the chaotic interval $\mathcal{A}$ as Milnor attractor on the x-axis. In the example shown in Fig. 10(a) at $b = 0.426$, it is $\Lambda_\perp^{\text{nat}} < 0$ and almost all the points without a divergent trajectory have the ω-limit set on the x-axis, in the chaotic interval $\mathcal{A}$, so that the Milnor attractor attracts almost all the points not belonging to $B(\infty)$.

For $b_{\text{blow}} < b < 0.44919772$ the internal fixed point P^* is still a saddle, and on the x-axis it is $\Lambda_\perp^{\text{nat}} > 0$ so that the stable set of the chaotic interval, i.e. the points having the ω-limit set on the x-axis, now constitute a set of zero measure (for example, related to the preimages of P_0 which are dense in the chaotic interval $[c_1, c]$, and similarly for the other transversely repelling cycles), and $\mathcal{A}$ is no longer a Milnor attractor. The effect of the blowout bifurcation at $b = b_{\text{blow}}$ is the appearance of a chaotic attracting set in the region $y > 0$ (while no attracting set is observed in the region $y < 0$). An example is shown in the enlargement of Fig. 10(b) at $b = 0.428$ (at which $\Lambda_\perp^{\text{nat}} > 0$) where almost all the points without a divergent trajectory have the ω-limit set consisting of a chaotic set which is very close, but not attached, to the x-axis, and it consists of two pieces, which are invariant for the second iterate of the map, T^2, as it is for the invariant set on the x-axis, since the invariant interval $\mathcal{A} = [c_1, c]$ consists of two intervals $[c_1, P_0]$ and $[P_0, c]$ with $P_0 = c_2$ invariant for the map $f^2(x)$.

This chaotic set seems a topological attractor, as it becomes more evident when increasing b, so that its area increases, as shown in Fig. 10(c) at $b = 0.439$, since an open neighborhood exists around it, belonging to its basin of attraction.

In both the examples shown in Figs. 10(b) and 10(c) the images of an arc of critical line LC_{-1} are shown, LC and LC_1 on the external boundaries

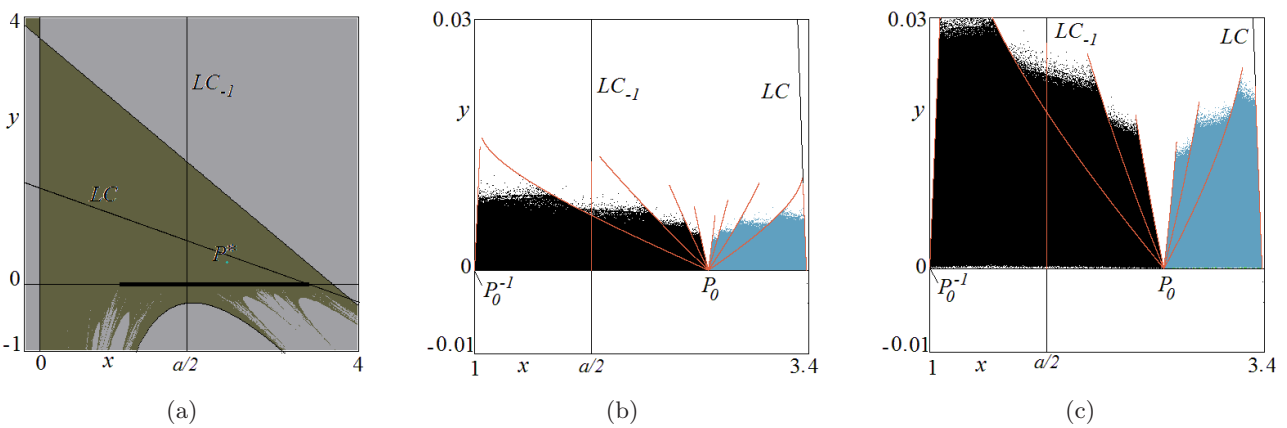

(a) (b) (c)

Fig. 10. Phase plane at $a = 3.67857351$, on the x-axis, the chaotic interval $\mathcal{A}$ is attracting for map $f(x)$. In (a) $b = 0.426$, after the riddling bifurcation, $\mathcal{A}$ is a Milnor attractor and attracts almost all the nondivergent trajectories. In (b) $b = 0.428$, the enlargement close to the x-axis, after the blowout bifurcation, $\mathcal{A}$ is no longer a Milnor attractor, its stable set is of zero measure, a chaotic attractor in two pieces is observed, which is invariant for the second iterate, map T^2, and the two pieces are shown in different colors. The images of an arc of critical line LC_{-1} are shown in red. In (c) $b = 0.439$, the enlargement close to the x-axis, shows a wider chaotic attractor in two pieces, invariant for map T^2, and the images of an arc of critical line LC_{-1} are shown in red.

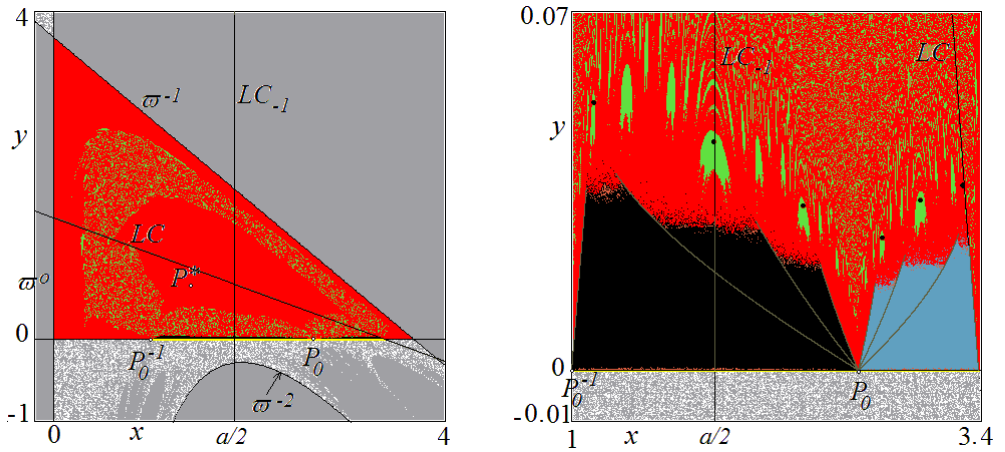

(a) (b)

Fig. 11. Phase plane at $a = 3.67857351, b = 0.44$, on the x-axis, the chaotic interval $\mathcal{A}$ is attracting for map $f(x)$, but its stable set for map T is of zero measure. In (a) there are two topological attractors, besides the chaotic attractor in two pieces, with basin in red, there is an attracting cycle of period 6 whose basin is shown in green, which are evidenced in the enlargement in (b).

of the chaotic set, while all the other images LC_n are issuing from the fixed point P_0, since this is the first homoclinic bifurcation of P_0, occurring when $f^3(c_{-1}) = c_2 = P_0$. The lower and upper boundaries of the chaotic attractor may be related to the unstable set of some saddle cycle.

This is the unique attracting set numerically observed when increasing b, up to a value at which a pair of internal 6-cycles appears via saddle-node, leading to a 6-cycle attracting node (before the bifurcation at $b = b_f$ leading to P^* attracting). An example of bistability is shown in Fig. 11 at $b = 0.44$.

The 6-cycle is still attracting at $b = 0.4405$ but no longer at $b = 0.441$. It is possible that other coexisting attractors appear before the bifurcation of the fixed point, although we have not observed them in our numerical simulations.

At $b = 0.45 > b_f$ the fixed point P^* is attracting, and the stable set of the internal saddle 2-cycle separates the two basins, P^* and the chaotic attractor. Now the chaotic attractor is larger, portions of its boundary are given by segments of critical lines LC_i, an area bounded from above can be easily obtained, while the lower part is now quite far from the x-axis, as shown in the enlargement of Fig. 12.

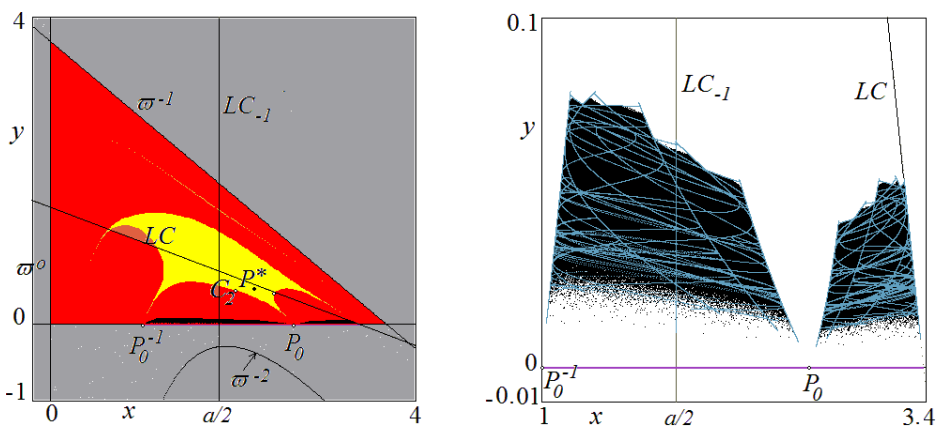

(a) (b)

Fig. 12. Phase plane at $a = 3.67857351, b = 0.45$, on the x-axis, the chaotic interval $\mathcal{A}$ is attracting for map $f(x)$, but its stable set for map T is of zero measure. In (a) there are two topological attractors, besides the chaotic attractor in two pieces, with basin in red, there is the attracting fixed point P^*, whose basin is in yellow. The two-piece chaotic attractor is evidenced in the enlargement in (b).

3.4. *Nontopological chaotic intervals as Milnor attractors*

In the examples mentioned above map T has the chaotic intervals which are true attractors of map $f(x)$, occurring at the merging of a pair of absorbing intervals (for map f^4, or f^2 or f). However, chaotic intervals also occur at an expansion bifurcation [Avrutin *et al.*, 2019] when the boundary of the intervals include a repelling cycle which undegoes a homoclinic bifurcation, the effect of the bifurcation is the transition to a wider absorbing interval. The values of the parameter a at which this occurs are accumulation points of several kinds of bifurcations [Mira, 1987]. Clearly, also in such a case Proposition 4 holds and at low values of b all the cycles in the chaotic intervals are transversely attracting, and thus the set of chaotic intervals is a Milnor attractor for map T for an interval of b values, and undergoes a blowout bifurcation with increasing b. Moreover, a peculiarity of such chaotic set is that in any neighborhood of any of its points, there are points which are mapped on the boundary, in the repelling cycle. This is due to the fact that at the expansion bifurcation the cycle on the border is an image of finite rank of the critical point $c_{-1} = a/2$ which, on its turn, has preimages which are dense in the chaotic intervals [Mira, 1987; Avrutin *et al.*, 2019].

In order to investigate a similar case we consider the value of a related to the homoclinic bifurcation of the 3-cycle of the logistic map, which bounds the immediate basin of the three-piece attracting set before the expansion bifurcation, occurring when the unstable 3-cycle merges with the critical point on the boundary of the absorbing intervals. This leads to three chaotic intervals having on the boundary an unstable 3-cycle on the x-axis, but transversely attracting at low values of b, and also all the cycles with periodic points dense in the chaotic intervals are transversely attracting. In our simulations we fix $a = 3.8568$, in the interval $0 < b < b_f$ the only observed attracting set is this Milnor attractor on the x-axis. In the interval $b_f < b < b_{\text{blow}}$ (i.e. as long as it is $\Lambda_{\perp}^{\text{nat}} < 0$) we have some attracting set in the triangle Δ and the Milnor attractor on the x-axis. The blowout bifurcation occurs approximately at $b_{\text{blow}} = 0.62 < b_{\text{NS}}$ when the attracting set is the fixed point P^* after which the stable set of the chaotic intervals becomes a set of zero measures, and the basin of attraction of the attracting set in Δ is left, besides the set of divergent trajectories.

One more interesting case occurs at $a = 4$, when the first homoclinic bifurcation of the fixed point in the origin occurs. The logistic map is chaotic in the interval $I = [0, 4]$, which is not an attracting interval, since the endpoints of the interval include a cycle repelling in the other direction, and in this case it belongs to the boundary of divergent trajectories.

3.4.1. *Transitions at $a = 4$*

For the particular case occurring at $a = 4$, on the x-axis we have a chaotic interval $I = [0, 4]$ (with periodic points dense in $[0, 4]$), which cannot be a topological attractor since in any neighborhood of any point of the interval there are points mapped into O in a finite number of iterations, as well as points having divergent trajectories. In fact, the first rank preimage of the vertical axis $x = 0$, ω^{-1} [given in (29)], intersects the x-axis exactly at the point with $x = 4$, so that, as we know, the endpoints are repelling from outside. Moreover, the arc of the preimage ω^{-2} [given in (31)] is tangent to the x-axis in the region $y \leq 0$ at the critical point c_{-1} ($x = 2$), and its preimages are also tangent to the x-axis in the region $y \leq 0$ in the preimages of the critical point c_{-1} which are dense in the chaotic interval $[0, 4]$. Thus, it can only be a Milnor attractor as long as its stable set is of positive measure, as it occurs when all the cycles existing in I are transversely attracting, at low values of b.

Also in this case, we have an interval of values of b in which the stable set of the chaotic interval, Milnor attractor, is not riddled in anything else, and attracts almost all the points having bounded trajectories, an example is shown in Fig. 13(a).

Increasing b, the first cycle which becomes transversely repelling most likely is the fixed point P_0 when it merges with P^*, which occurs at $b = b_0 = 1/3$. The fixed point P^* becomes attracting at $b = b_f = 0.42857142857$, and undergoes the NS bifurcation at $b = b_{\text{NS}} = 2/3$. For $0 < b < b_f$ we have detected only trajectories converging to the Milnor attractor (i.e. the stable set is not riddled into another basin of attraction), while for $b_f < b < b_{\text{NS}}$ we have a topological attractor (the fixed point P^*) and a Milnor attractor on the x-axis, as shown in Fig. 13(b), the stable set of I is riddled into the basin of attraction $B(P^*)$.

After the NS bifurcation of P^* we have some other topological attractor [an example is shown

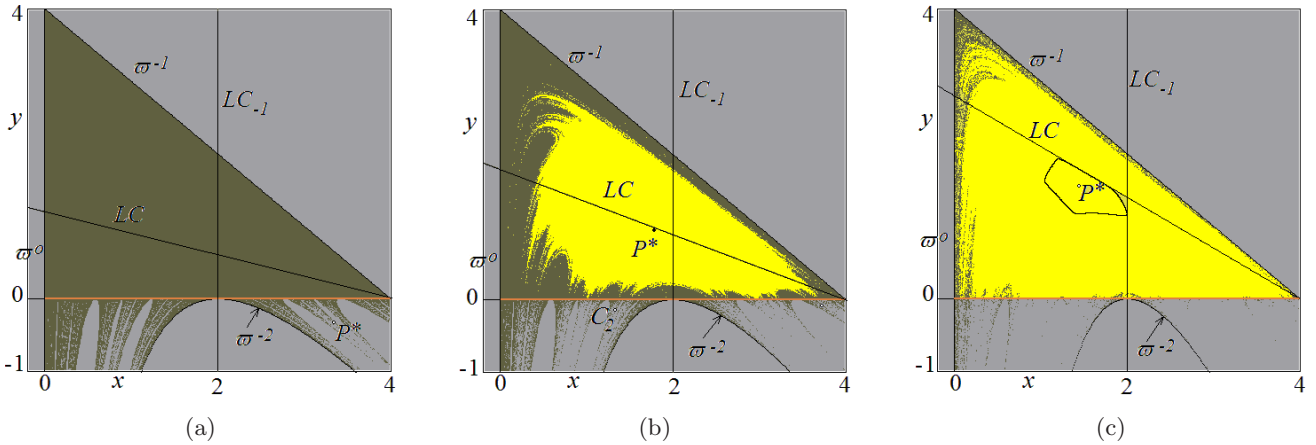

Fig. 13. Phase plane at $a = 4$, on the x-axis the chaotic interval $I = [0, 4]$ is not an attractor for map $f(x)$. In (a) $b = 0.3$, I is a Milnor attractor and attracts almost all the nondivergent trajectories. In (b) $b = 0.45$, I is a Milnor attractor and attracts a set of positive measure, and there is the attracting fixed point P^*, whose basin is in yellow. In (c) $b = 0.7$, after the NS bifurcation of P^* the attractor is a closed invariant curve.

in Fig. 13(c)], which becomes a chaotic attracting set quite large in dimensions, and approaches the boundary of its basin of attraction. That is, for $b > b_{\rm NS}$ as long as another attracting set coexists with I, Milnor attractor, we have that the stable set of I is riddled into the basin of another attracting set, which becomes a chaotic area as b increases.

A contact bifurcation occurs between the chaotic area and the boundary of its basin of attraction at a value of b very close to the example shown in Fig. 14(a), after which we have a chaotic repeller in Δ and again almost all the points are attracted to the x-axis [see Fig. 14(b)] which is still a Milnor attractor.

The dynamics are the same up to $b = 1$ when the critical line LC merges with the preimage ω^{-1} and the triangle Δ becomes invariant. The particular case $(a, b) = (4, 1)$ has been investigated in several papers, and still it has not been proved that the set of points having the ω-limit set on the x-axis is a set of zero Lebesgue measures, but we conjecture that this is true and that the blowout bifurcation occurs exactly at $b = 1$, after which almost all the trajectories are divergent. However, the chaotic interval $I = [0, 4]$ is not a chaotic saddle. In fact, in [Gardini & Tikjha, 2020] it is evidenced that there are still many cycles on the x-axis which are transversely attracting, not only at $b = 1$ but also at

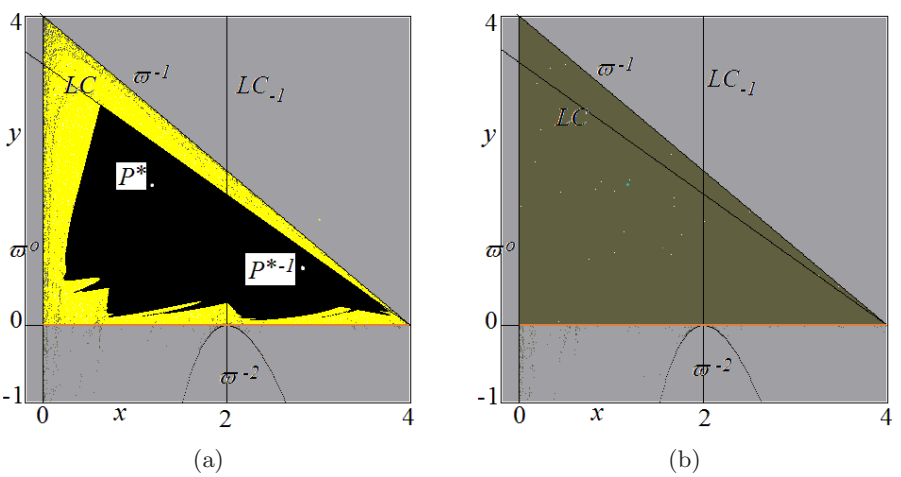

Fig. 14. Phase plane at $a = 4$, on the x-axis the chaotic interval $I = [0, 4]$ is not an attractor for map $f(x)$. In (a) $b = 0.84374$, I is a Milnor attractor and the topological attractor is a chaotic area, close to the boundary of its basin of attraction (in yellow). In (b) $b = 0.85$, after the contact bifurcation a chaotic repeller is left and the Milnor attractor I attracts almost all the nondivergent trajectories.

$b \neq 1$, for example, all the maximal cycles having symbolic sequence RL^n for any $n > 2$.

It is interesting to investigate the particular role played by the maximal cycles having symbolic sequence RL^n for $n \geq 2$ not only at $b = 1$ but as b increases from 0, as considered in Sec. 5.

However, let us first remark that the peculiar behavior after a riddling bifurcation associated with a stable set not riddled into some other basin of attraction is not a rare phenomenon, since it may occur also for the bifurcation of cycles, as evidenced in the next section.

4. Milnor Attractors Related to Attracting Cycles of Map T

In the previous section, we have seen that Milnor attractors are common, increasing b, whenever the parameter a of the logistic map corresponds to chaotic intervals, and it is known that the set of values of a at which this occurs is a set of positive measure [Jacobson, 1981; Thunberg, 2001]. For each fixed value of a there exists an interval of values b at which the chaotic set on the x-axis is a topological or Milnor attractor for map T. However, there are values of a at which also the logistic map $f(x)$, as a one-dimensional map on the x-axis, has a Milnor attractor. In fact, this happens for $a_\infty < a < 4$ at any fold (or tangent) bifurcation of the map, when the graph of the function $f^n(x)$ becomes tangent to the diagonal (leading to an attracting cycle and a repelling one). At the fold bifurcation the two n-cycles are merging into a unique n-cycle, say $\mathcal{C}_n^*$, which is attracting from one side and repelling from the other side (where it also has homoclinic points), so that it is not a topological attractor, but it attracts almost all the points of the interval $[0, a]$, and thus it is a Milnor attractor for $f(x)$.

The question is if such a cycle (at the fold bifurcation) is a Milnor attractor also for map T. And the answer is yes, as long as it is transversely attracting. Thus, denoting $\{x_1^*, \ldots, x_n^*\}$ as the periodic points of the cycle $\mathcal{C}_n^*$ at the fold bifurcation value, we see a Milnor attractor of map T as long as $\lambda_{n,\perp}(\mathcal{C}_n^*) < 1$, which occurs (from Proposition 4) for

$$0 < b < \frac{1}{\left(\prod_{i=1}^{n} x_i^*\right)^{1/n}}. \tag{33}$$

So, for such transitions, we have Milnor attractors which are robust, or persistent, with respect to the parameter b (although not with respect to the parameter a).

Differently, in the examples given in the following, the attractors are not robust, because they are related (for each value of a) to the bifurcation value of b giving $\lambda_{n,\perp} = 1$.

We know that the values of the parameter a at which we have an attracting cycle for the logistic map lead to a set of positive measures (since it is the union of open intervals of values). For each fixed value of a of this kind we know that at low values of b such an n-cycle is also a topological attractor for map T, and that it becomes transversely repelling at the bifurcation $\lambda_{n,\perp} = 1$. Thus, is it possible that at the bifurcation value the n-cycle on the x-axis becomes a Milnor attractor?

Here we have no unique answer because it depends on the kind of cycle which is merging with that on the x-axis, there are examples in which the answer is yes (some evidences are given below and in the next section), and other cases in which it is no.

For example, for a fixed value $a \in (1, 3)$ at which the fixed point P_0 is attracting on the x-axis, the transverse direction becomes repelling at the bifurcation $\mathcal{P}(1) = 0$, when the fixed point P^* (saddle) from the region $y < 0$ merges with it and then enters the region $y > 0$ as an attracting node. In all such cases, at the bifurcation value $b = b_0$ the fixed point $P_0 = P^*$ repels points in the region $y < 0$ while it attracts points in the region $y > 0$, from the triangle Δ, in a set of positive measures, and thus it is a Milnor attractor (an example is given in Sec. 2.4).

Differently, for $a > 3$, when the attracting set on the x-axis is the 2-cycle flip bifurcated from P_0, then the bifurcation in the transverse direction of this topological attractor occurs when the saddle 2-cycle $\mathcal{C}_2$ flip bifurcated from P^* merges with the 2-cycle on the x-axis from the region $y > 0$, at $b = \frac{1}{\sqrt{1+a}}$ (from Proposition 2). After the transverse bifurcation the 2-cycle in the region $y < 0$ is a repelling node. At the bifurcation value the resulting cycle is not a Milnor attractor, since the transverse direction in the region $y > 0$ leads the points to converge to the attracting fixed point P^* while those of the transverse direction in the region $y < 0$ leads the points to a divergent trajectory.

However, in the cases of the attracting cycles with period 2^n for $n > 1$ before the Feigenbaum point a_∞, we conjecture that at the transverse bifurcation, we always have a Milnor attractor. This is due to the fact that the transition of the eigenvalue from $\lambda_{2^n,\perp} < 1$ to $\lambda_{2^n,\perp} > 1$ seems to occur with a saddle 2^n-cycle which from the region $y < 0$ enters the region $y > 0$ becoming an attracting node (as we have shown in the example with the 2^3-cycle in Sec. 2.5), which implies that at the bifurcation, when $\lambda_{2^n,\perp} = 1$, the x-axis still has an attracting set of positive measures from points of the triangle Δ.

5. Milnor Attractors Related to the Transverse Bifurcation of Attracting Maximal Cycles

It is interesting to investigate the particular role played by the maximal cycles having symbolic sequence RL^n for $n \geq 2$ which occur at values of a close to 4, in particular for the cases with $n \geq 3$ because we know (see [Gardini & Tikjha, 2020]) that the bifurcation related to the transverse eigenvalue occurs at values $b > 1$ which means that the basin of divergent trajectories $B(\infty)$ is dominant in the triangle Δ. In fact, from the equations of the straight lines LC in (7) and ω^{-1} in (29) it follows that for any fixed value of a, for $b > 4/a$ the basin $B(\infty)$ of divergent trajectories intersects the triangle Δ and the portion between ω^{-1} and LC has infinitely many preimages in Δ, because the stable set of the origin is expanded inside it, and thus also the basin of divergent trajectories. Often, this is a kind of "final bifurcation" which leads to divergence for almost all the points in Δ, but it is not true in our case, as described in this section, through some examples.

We describe the dynamics occurring at the transverse bifurcation of the attracting 3-cycle RL^2, the attracting 4-cycle RL^3 and the 8-cycle flip bifurcated from it, which seem related to Milnor attractors (but only at the transverse bifurcation value). What characterizes the different dynamic behavior of RL^n for $n = 2$ and $n > 2$ is that the transverse bifurcation of the 3-cycle occurs when there exists a topological attracting set in the triangle Δ, while for all the other cycles with $n > 2$ (and also for the related cycles obtained via flip bifurcations from them) when the transverse bifurcation occurs (and it is for $b > 1$) there are no attracting sets internal to the triangle Δ, but mainly divergent trajectories.

It is clear that a dynamic behavior similar to the one shown below may occur for any other maximal cycle RL^n, $n > 2$.

5.1. *Transverse bifurcation of the attracting 3-cycle RL^2*

Let us consider fixed the value $a = 3.83$ so that on the x-axis there is an attracting 3-cycle, which is also transversely attracting for $b < 0.6179$ (from $\lambda_{3,\perp} = b^3 \prod_{i=1}^{3} x_i < 1$ and $\prod_{i=1}^{3} x_i = 4.238775261$), and thus the 3-cycle is a topological attractor also for the two-dimensional map T. In Fig. 15(a) we show the immediate basin of the periodic point of the 3-cycle close to the critical point $a/2$ for the

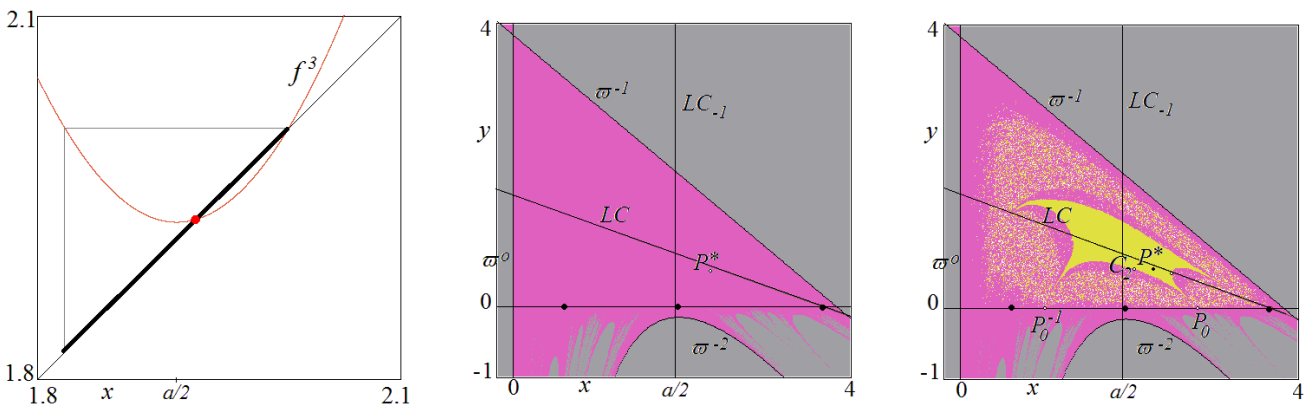

Fig. 15. Parameter $a = 3.83$. In (a) enlargement of $f^3(x)$ in a neighborhood of $c_{-1} = a/2$ evidencing the immediate basin of a point of the attracting 3-cycle on the x-axis. In (b) $b = 0.43$, the 3-cycle on the x-axis is the only attractor of map T, its basin is in pink. In (c) $b = 0.44$, two attractors of map T coexist, the 3-cycle on the x-axis (basin in pink) and the attracting fixed point P^* (basin in yellow).

third iterate of the logistic map, leading to the immediate basin on the x-axis for the logistic map, whose global basin has however a fractal structure, that is, the frontier includes a chaotic repeller. It seems the only attractor of T up to the stability of P^*. Here P^* enters the region $y > 0$ at $b = b_0 = 0.35335689$ and becomes attracting at $b = b_f = 0.439238653$.

In Fig. 15(b) the 3-cycle on the x-axis is the unique attractor, although a chaotic repeller exists, not only on the x-axis, but also inside the triangle Δ. This can be observed numerically when P^* becomes attracting, an example with the two topological attractors is shown in Fig. 15(c) at $b = 0.44$, where the fractal structure of the two basins (due to a chaotic repeller inside Δ) can be seen.

Increasing the parameter b the basin of the attracting fixed point P^* becomes larger, while the basin of the attracting 3-cycle decreases more and more. Recall that increasing b only the transverse eigenvalue changes, thus the 3-cycle persists as a topological attractor as long as $\lambda_{3,\perp} < 1$ and thus up to $b = 0.6179$ at which a transcritical bifurcation occurs. For $b < 0.6179$ close to the transverse bifurcation a saddle 3-cycle exists in the region $y > 0$ belonging to the boundary of the basin of attraction of the 3-cycle, an example is shown in Fig. 16 and the two 3-cycles are evidenced in the enlargement (the attracting one on the x-axis and the saddle one on the basin boundary).

At $b = 0.6179$ the two 3-cycles merge on the x-axis, and the transverse direction is repelling in the region $y > 0$ (where the points converge to the attracting fixed point P^*) but it is attracting in the region $y < 0$ and we have numerical evidence that the set of points whose trajectory converges to the 3-cycle on the x-axis is a set of positive measure, so that we conjecture that it is a Milnor attractor.

For $b > 0.6179$ the 3-cycle on the x-axis is a saddle, transversely repelling, but the bifurcation leads to the appearance of an attracting 3-cycle in the region $y < 0$, an example is shown in Fig. 17 and in the enlargement the two cycles of period 3 are evidenced. Now the stable set of the saddle 3-cycle on the x-axis also for map T is restricted to the interval $[0, a]$. The x-axis separates points having different behavior in the regions above and below the x-axis itself. In fact, in the region $y > 0$ in Δ the points converge to the attracting fixed point P^* while in the region $y < 0$ the points either converge to the new attracting 3-cycle of T or diverge.

5.2. *Transverse bifurcation of the attracting 4-cycle* $\mathbf{RL^3}$

A different behavior can be seen at $a = 3.9603$ when there exists an attracting 4-cycle RL^3 of the logistic map, which is transversely attracting for $b < 1.0926482984745$ (for which $\lambda_{4,\perp} < 1$), and it is a topological attractor also for map T. In Fig. 18(a) we show the immediate basin of the fourth iterate of the logistic map of the periodic point of the 4-cycle close to the critical point $a/2$, leading to the immediate basin on the x-axis for the logistic map, whose global basin has however a fractal structure, and also for the two-dimensional map T, as shown

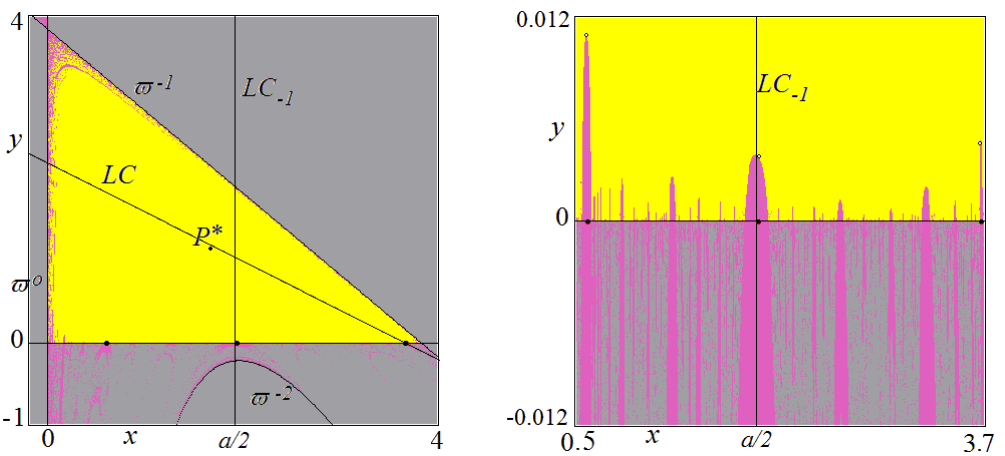

(a) (b)

Fig. 16. Parameters $a = 3.83, b = 0.6$. In (a) the two attractors of map T still coexist, the basin of the 3-cycle (in pink) is smaller in size, the basin of P^* is in yellow. The enlargement in (b) shows a saddle 3-cycle on the basin boundary of the attracting 3-cycle, before the bifurcation related to the transverse eigenvalue.

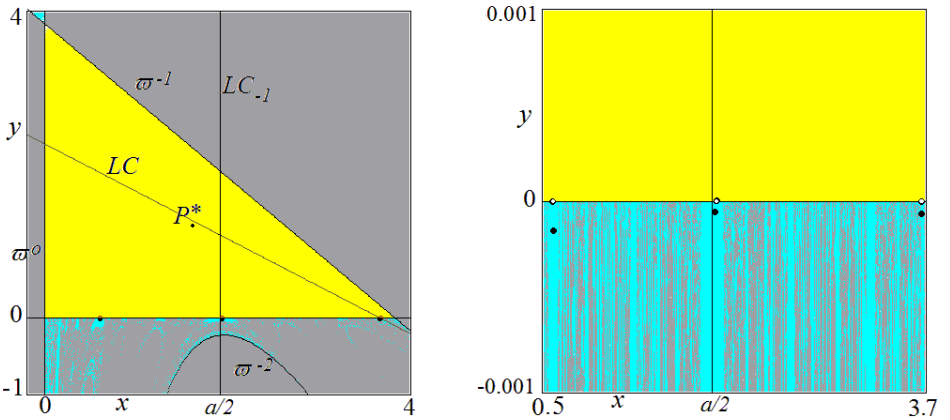

(a) (b)

Fig. 17. Parameters $a = 3.83$, $b = 0.618$. In (a) after the bifurcation related to the transverse eigenvalue, two attractors of map T coexist, the attracting fixed point P^* (basin in yellow), and the 3-cycle in the region $y < 0$ (basin in azure). The enlargement in (b) shows the attracting 3-cycle and the saddle 3-cycle on the x-axis.

in Fig. 18(b) where the fractal structure is evident in the region $y < 0$. It seems the only attractor of T up to the stability of P^*. Here P^* enters the region $y > 0$ at $b = b_0 = 0.3378036$ and becomes attracting at $b = b_f = 0.4310159$.

In Fig. 18(b) the 4-cycle is the unique attractor, although a chaotic repeller exists on the x-axis, and it may also exist inside the triangle Δ. When P^* becomes attracting, there are two coexisting topological attractors (P^* and the 4-cycle), an example is shown in Fig. 18(c) at $b = 0.44$.

There are two coexisting topological attractors also in Fig. 19(a), after the NS bifurcation of P^* (occurring at $b = b_{\rm NS} = 0.3378036$) but now the attractors are a closed invariant curve and the 4-cycle is on the x-axis, the enlargements evidence the fractal structure of the basin of the 4-cycle.

There are coexisting topological attractors also in the many bifurcations occurring (for increasing b) near the closed invariant curve leading to chaotic attractors. The example shown in Fig. 20(a) evidences that the chaotic attractor is close to the boundary of its basin of attraction (separating this basin from that of the attracting 4-cycle on the x-axis) and thus close to having a contact bifurcation with the frontier.

The contact leads to a chaotic repeller, leaving as unique topological attractor the 4-cycle on the x-axis. Figure 21 seems like a compact basin, but it is not, inside it the former attractor has a chaotic

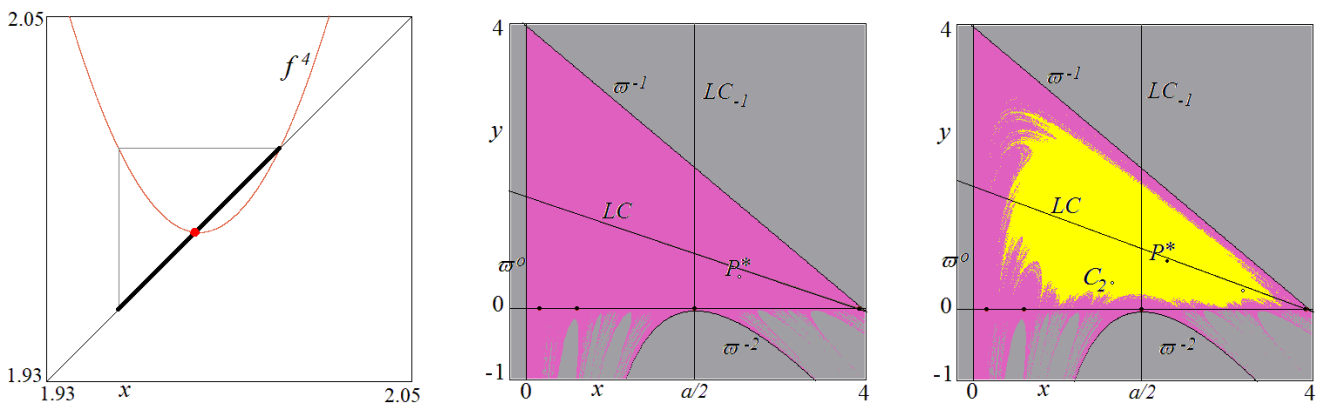

(a) (b) (c)

Fig. 18. Parameter $a = 3.9603$. In (a) enlargement of $f^4(x)$ in a neighborhood of $c_{-1} = a/2$ evidencing the immediate basin of a point of the attracting 4-cycle on the x-axis. In (b) $b = 0.4$, the 4-cycle on the x-axis is the only attractor of map T, its basin is in pink. In (c) $b = 0.44$, two attractors of map T coexist, the 4-cycle on the x-axis (basin in pink) and the attracting fixed point P^* (basin in yellow).

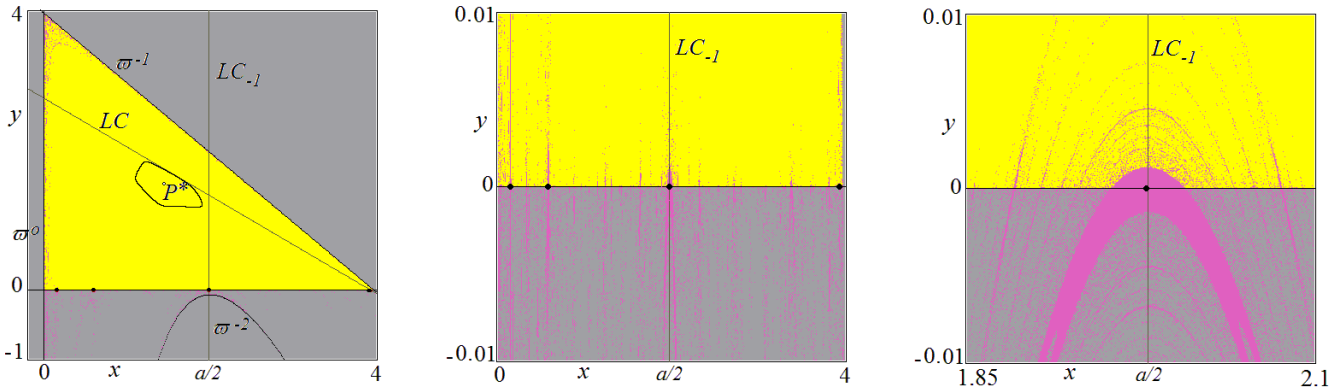

(a) (b) (c)

Fig. 19. Parameters $a = 3.9603, b = 0.7$. In (a) two attractors of map T coexist, the 4-cycle on the x-axis (basin in pink) and the attracting closed invariant curve after the NS bifurcation of P^* (basin in yellow). In (b) enlargement of a strip around the x-axis. In (c) enlargement of a strip of (b) around the critical point c_{-1}.

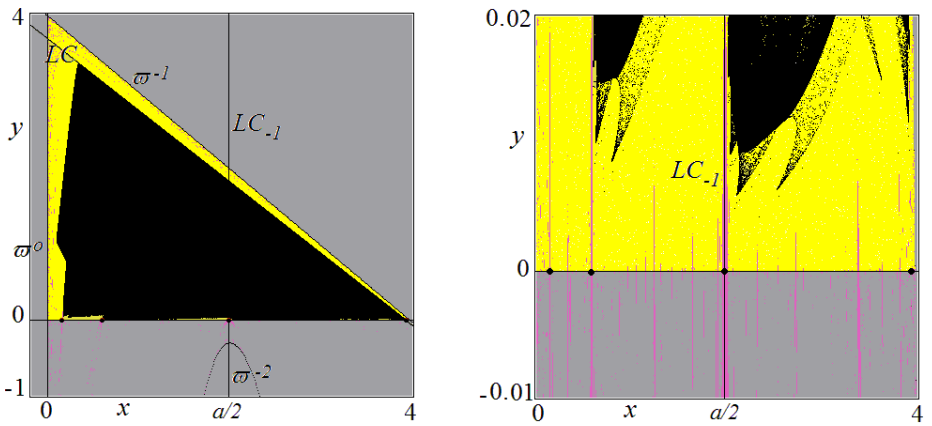

(a) (b)

Fig. 20. Parameters $a = 3.9603, b = 0.933$. In (a) two attractors of map T coexist, the 4-cycle on the x-axis (basin in pink) and a chaotic area (basin in yellow) close to a contact with the frontier of its basin boundary. In (b) enlargement of a strip around the x-axis.

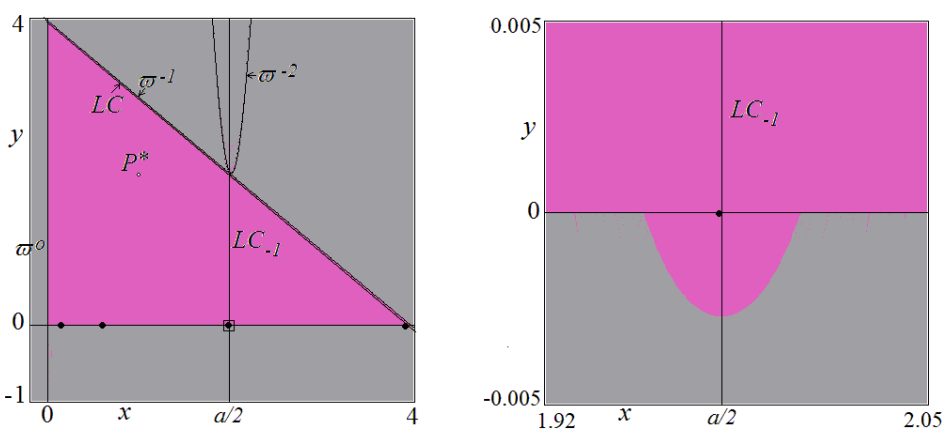

(a) (b)

Fig. 21. Parameters $a = 3.9603, b = 1.01$. In (a) the 4-cycle on the x-axis is again the only attractor of map T, its basin is in pink. The preimage ω^{-2} of the origin is near the crossing of ω^{-1} and LC. In (b) enlargement of the rectangle shown in (a) around the critical point c_{-1}.

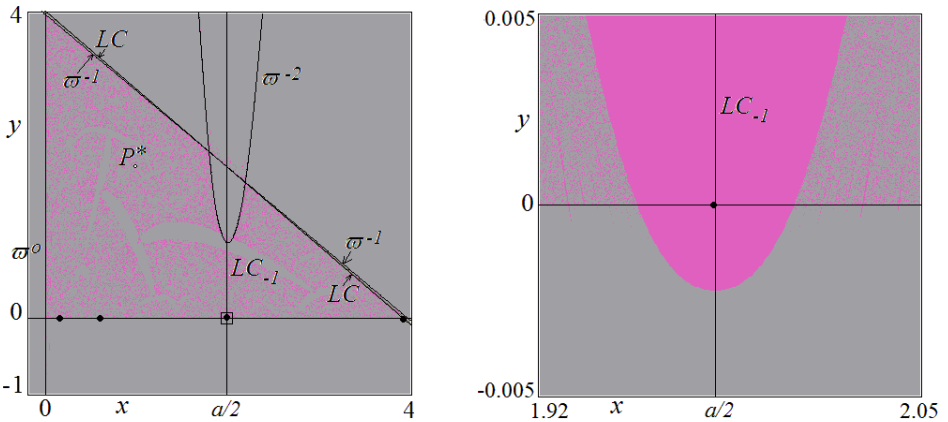

(a) (b)

Fig. 22. Parameters $a = 3.9603$, $b = 1.02$. In (a) the 4-cycle on the x-axis is the only attractor of map T, its basin is in pink, but the majority of the points in Δ have divergent trajectories. In (b) enlargement of the rectangle shown in (a) around the critical point c_{-1}.

repeller left. In the enlargement it can be seen that in the region $y < 0$ the basin has a saddle 4-cycle on the boundary of the immediate basin. In Fig. 21(a) we can also see that the preimage ω^{-2} of the y-axis, bounding the divergent trajectories, is close to the upper limit of the basin (given by ω^{-1}), and when ω^{-2} crosses the critical line LC we have an explosion of the stable set $W^S(O)$ separating the basin of the attractor from the points having divergent trajectories, as shown in Fig. 22(a) whose enlargement evidences that the 4-cycle is still a topological attractor for map T.

Increasing b the basin of the 4-cycle decreases, as shown in Fig. 23, and it remains a topological attractor up to the bifurcation related to the transverse eigenvalue, which now occurs with a saddle 4-cycle (on the basin boundary) approaching the x-axis from the region $y < 0$.

At the bifurcation $\lambda_{4,\perp} = 1$ the two 4-cycles merge on the x-axis, and the transverse direction is repelling in the region $y < 0$ (where the points have divergent trajectories) but it is attracting in the region $y > 0$ and from the numerical simulations we conjecture that the set of points whose trajectory converges to the 4-cycle on the x-axis is a set of positive measures, so that it is a Milnor attractor.

After the bifurcation, the 4-cycle on the x-axis becomes a saddle while an attracting 4-cycle node appears in the region $y > 0$, so that another topological attractor is created, whose basin is evidenced in red in Fig. 24, and it has positive Lebesgue

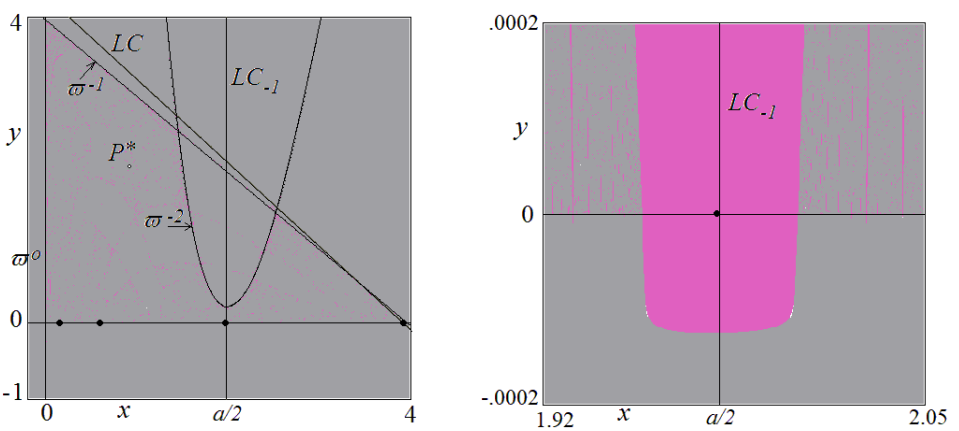

(a) (b)

Fig. 23. Parameters $a = 3.9603, b = 1.092$. In (a) the 4-cycle on the x-axis is the only attractor of map T, its basin in pink becomes smaller and smaller, the majority of the points in Δ have divergent trajectories. In (b) enlargement of a small portion of (a) around the critical point c_{-1}, showing that the 4-cycle is close to the bifurcation related to the transverse eigenvalue.

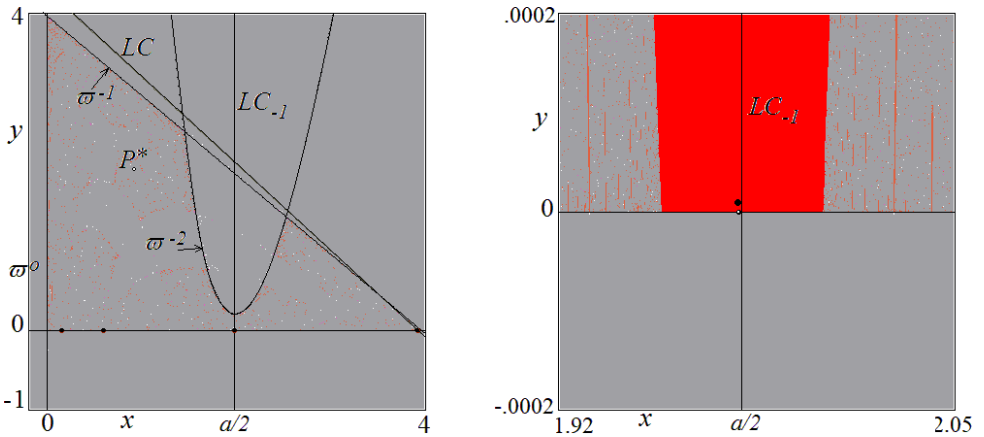

Fig. 24. Parameters $a = 3.9603, b = 1.09269$. In (a) the 4-cycle on the x-axis is a saddle transversely repelling, the only attractor of map T is a 4-cycle in the region $y > 0$, its basin is in red, the majority of the points in Δ have divergent trajectories. In (b) enlargement of a small portion of (a) around the critical point c_{-1}.

measure, attracting points of the triangle Δ, even if the largest part of points in Δ have divergent trajectories, as shown in Fig. 24.

5.3. *Transverse bifurcation of the attracting 8-cycle*

It is well known that from each cycle RL^n for $n \geq 3$ a cascade of period-doubling bifurcations occur, all leading to topological attractors of map T at least for low values of b, and for all of them a transition similar to the one described above for the 4-cycle may occur. We only comment here the bifurcations associated with the 8-cycle (flip bifurcated from the 4-cycle of the previous subsection at $a \simeq 3.9603$). Let us consider $a = 3.961$ fixed, at which there exists an attracting 8-cycle of the logistic map, which is also transversely attracting for $b < 1.0981667422$ (obtained from the related condition $\lambda_{8,\perp} < 1$), so that it is a topological attractor for the two-dimensional map T. In Fig. 25(a) we show an enlargement of the eighth iterate of the logistic map close to the critical point $a/2$, and the immediate basin of the periodic points of the 8-cycle close to the critical point, leading to the immediate basin of the logistic map on the x-axis. It seems the only attractor of T up to the stability of P^* occurring at $b = b_f = 0.43097256$, an example of bistability with

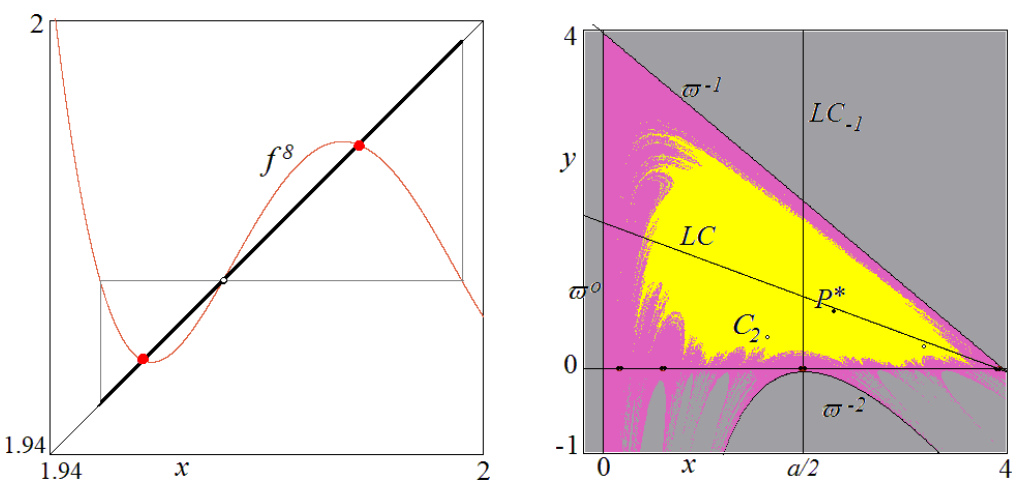

Fig. 25. Parameter $a = 3.961$. In (a) enlargement of $f^8(x)$ in a neighborhood of $c_{-1} = a/2$ evidencing the immediate basin of two points of the attracting 8-cycle on the x-axis which is also an attractor of map T. In (b) $b = 0.44$, two attractors of map T coexist, the 8-cycle on the x-axis (basin in pink) and the attracting fixed point P^* (basin in yellow).

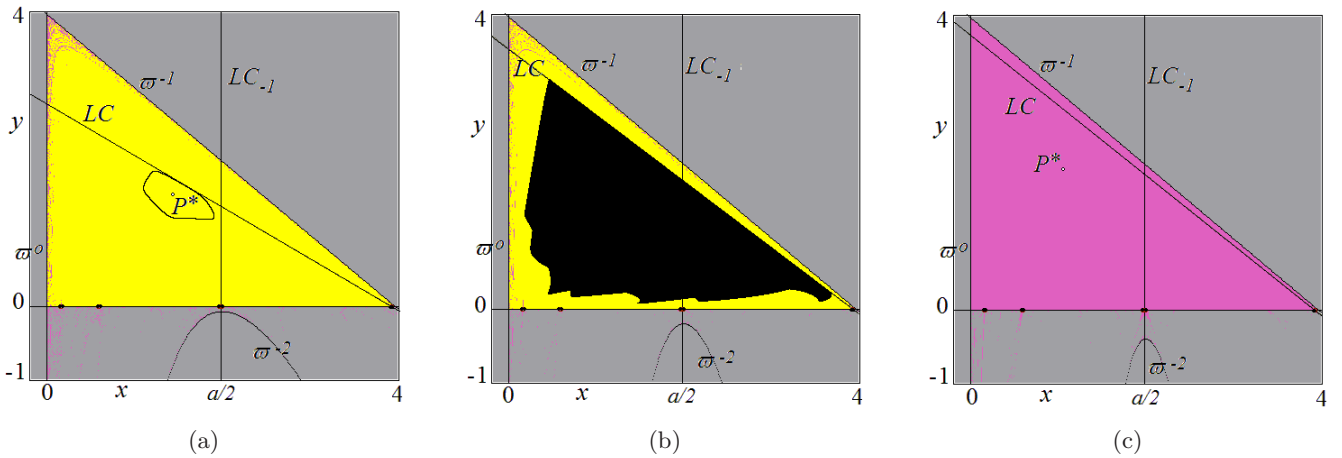

Fig. 26. Parameter $a = 3.961$. In (a) $b = 0.7$, two attractors of map T coexist, the 8-cycle on the x-axis (basin in pink) and an attracting closed invariant curve, after the NS bifurcation of P^* (basin in yellow). In (b) $b = 0.9$, two attractors of map T coexist, the 8-cycle on the x-axis (basin in pink) and chaotic attractor (basin in yellow). In (c) $b = 0.95$, after the contact bifurcation the only attractor of map T is the 8-cycle on the x-axis (basin in pink).

P^* is shown in Fig. 25, while the NS bifurcation occurs at $b = b_{\rm NS} = 0.675447484$.

Two (at least) topological attractors, one inside the triangle Δ and one on the x-axis, exist up to the contact bifurcation of the chaotic attractor (existing after the NS bifurcation of P^*) with the boundary of its basin of attraction, see Figs. 26(a) and 26(b), after which almost all the points belong to the basin of the attracting 8-cycle on the x-axis, as shown in Fig. 26(c).

As in the previous case one more relevant bifurcation occurs when Δ is no longer mapped into itself, changing drastically the structure of the basin of attraction of the 8-cycle. The preimages of the line $x = 0$ enter the triangular region Δ from above and then crossing LC there is an expansion of the stable set $W^S(O)$, at the same time expanding the area of points in Δ having divergent trajectories, as shown in Fig. 27 and its enlarged portion.

However, it is interesting to see that also in these situations, map T can still have two coexisting topological attractors, as shown in Fig. 28. The enlargement clearly evidences the existence of a chaotic attractor in eight pieces (only two of which are shown in the enlargement), when the 8-cycle on the x-axis is still a topological attractor of T. Thus, even if in the triangular region Δ the majority of the points have a divergent trajectory [as shown in

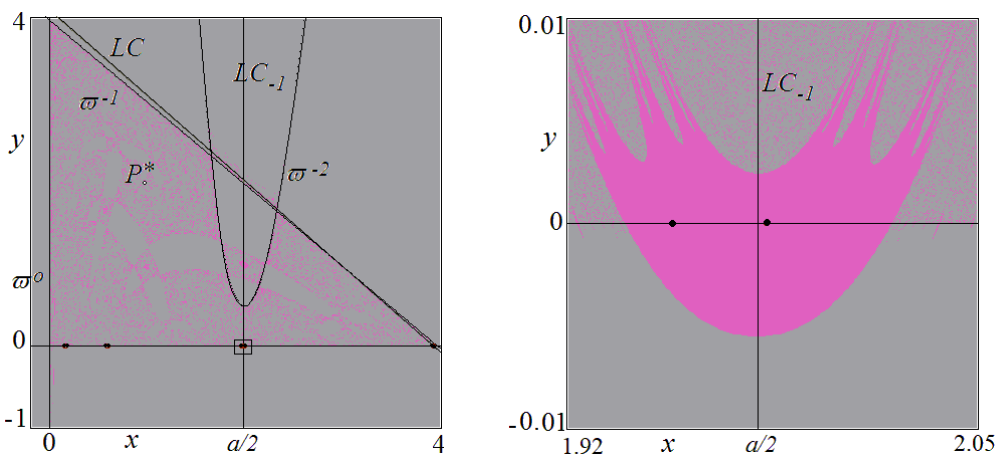

Fig. 27. Parameters $a = 3.9603, b = 1.04$. In (a) the 8-cycle on the x-axis is the only attractor of map T, its basin in pink is very small (but of positive measure), the majority of the points in Δ have divergent trajectories. In (b) enlargement of the rectangle shown in (a) around the critical point c_{-1}.

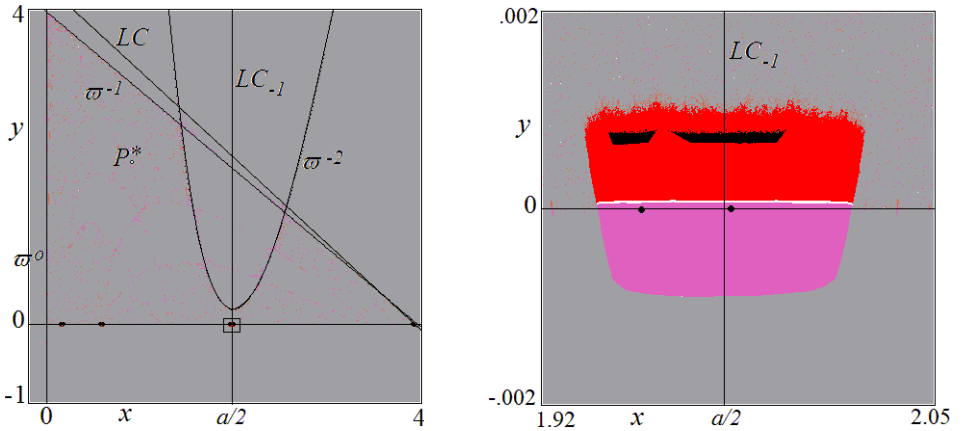

(a) (b)

Fig. 28. Parameters $a = 3.9603, b = 1.0981$. In (a) two topological attractors of map T coexist, with very small basins, the 8-cycle on the x-axis (its basin is in pink) and a chaotic attractor in eight cyclical pieces (with basin in red), the majority of the points in Δ have divergent trajectories. In (b) enlargement of the rectangle shown in (a) around the critical point c_{-1}, showing that the 8-cycle is close to the bifurcation related to the transverse eigenvalue.

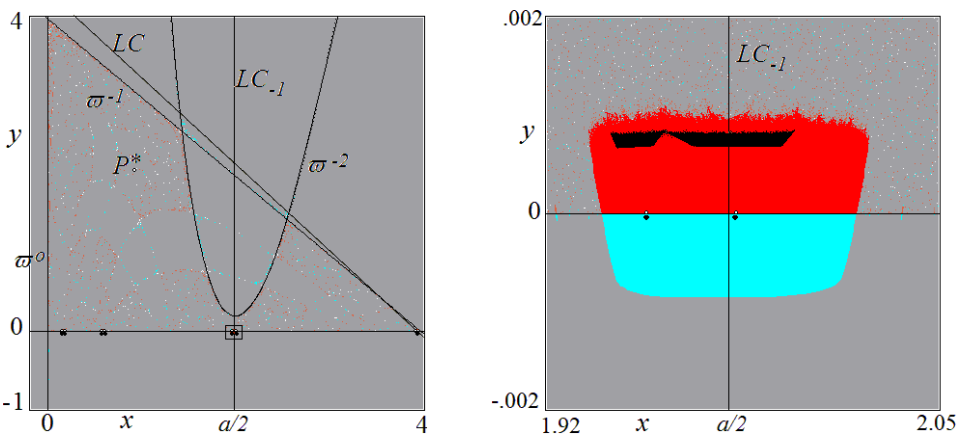

(a) (b)

Fig. 29. Parameters $a = 3.9603, b = 1.0982$. In (a) two topological attractors of map T coexist, with very small basins, an 8-cycle in the region $y < 0$ after the bifurcation related to the transverse eigenvalue (its basin is in azure) and a chaotic attractor in eight cyclical pieces (with basin in red), the majority of the points in Δ have divergent trajectories. In (b) enlargement of the rectangle shown in (a) around the critical point c_{-1}.

Fig. 28(a)], there are still two sets of positive measure, basins of attraction of two topological attractors. The bifurcation in the transverse direction of the 8-cycle on the x-axis occurs with its merging with an 8-cycle saddle from the region $y > 0$, which becomes an 8-cycle attracting node in the region $y < 0$ after the bifurcation, for $b > b_{8,\perp}$, thus still keeping two topological attractors, as shown in Fig. 29. Also in this example, at the transverse bifurcation occurring at $b = b_{8,\perp}$ the 8-cycle on the x-axis is repelling in the region $y > 0$, but attracting in the region $y < 0$, and numerically it seems to be a Milnor attractor with a stable set similar to the one existing for $b > b_{8,\perp}$ for the new 8-cycle in the region $y < 0$.

6. Conclusions

In this work, we have investigated some bifurcations related to the family of Lotka–Volterra maps $(x', y') = T(x, y) = (x(a - x - y), bxy)$ for $a > 1$ and $b > 0$. The recent literature is mainly focused on attracting sets belonging to the triangle Δ in the positive quadrant of the plane. However, the

existence of an invariant set on the x-axis leads to unexpected dynamic behaviors, related to both topological and Milnor attractors on the x-axis. We have evidenced some properties of map T, among which those related to a 2-cycle not belonging to the x-axis, the stable set of the origin O which belongs to the boundary of $B(\infty)$, showing that for any $a \in (1, 4]$ at low values of b the set existing in the interval $[0, a]$ of the x-axis is attracting (as topological or Milnor attractor). In particular, we have considered in Sec. 3 cases in which the set on the x-axis consists of chaotic intervals (attracting or not) and the related riddling and blowout bifurcations, mainly via numerical simulations, in order to show the dynamic result of these global bifurcations. Persistent cases of Milnor attractors are also associated with standard bifurcations of cycles on the x-axis, as shown in Sec. 4. Many results are not rigorously proved, and given as conjectures, since we do not have enough instruments for an exact evaluation. In particular, this happens with the outcomes of Milnor attractors related to cycles which are topological attractors both of map $f(x)$ and map T, as described in Sec. 5, in which the bifurcation in the transverse direction leads to topological attractors of map T in the region $y > 0$ or $y < 0$ in a context in which the majority of the trajectories are diverging.

Several others properties of map T are worth to be investigated further. For example, we have not given space to the NS bifurcation of the internal fixed point P^*, to the coexistence of attracting sets inside the triangle Δ and to the snapback repeller bifurcations of P^* and other internal cycles, which are also interesting to study that we leave for future work.

Acknowledgments

The work of L. Gardini has been done within the activities of the research project on "Models of behavioral economics for sustainable development" of the Department DESP of the University of Urbino. The work of W. Tikjha is supported by the Centre of Excellence in Mathematics, National Research Council of Thailand, Thailand Science Research and Innovation and Pibulsongkram Rajabhat University, and the author is grateful to the University of Urbino for the hospitality during his period of visit. This project is funded by National Research Council of Thailand (NRCT) — NRCT5-RSA63016-01.

References

Alexander, J., Yorke, J. A., You, Z. & Kan, I. [1992] "Riddled basins," *Int. J. Bifurcation and Chaos* **2**, 795–813.

Ashwin, P., Buescu, J. & Stewart, I. [1996] "From attractor to chaotic saddle: A tale of transverse instability," *Nonlinearity* **9**, 703–773.

Avrutin, V., Gardini, L., Sushko, I. & Tramontana, F. [2019] *Continuous and Discontinuous Piecewise-Smooth One-Dimensional Maps* (World Scientific, Singapore).

Balibrea, F., Guirao, J. L. G., Lampart, M. & Llibre, J. [2006] "Dynamics of a Lotka–Volterra map," *Fundamenta Mathematicae* **191**, 265–279.

Bischi, G. I., Gardini, L. & Mira, C. [1999] "Plane maps with denominator. Part I: Some generic properties," *Int. J. Bifurcation and Chaos* **9**, 119–153.

Buescu, J. [1997] *Exotic Attractors*: *From Liapunov Stability to Riddled Basins* (Birkhauser, Basel).

Devaney, R. L. [1989] *An Introduction to Chaotic Dynamical Systems* (Addison-Wesley, Reading).

Gardini, L. & Tikjha, W. [2020] "Bifurcations in a one-parameter family of Lotka–Volterra 2D transformations", Submitted for publication. The Working paper which can be downloaded from https://www.researchgate.net/publication/340172422_Bifurcations_in_a_one-parameter_family_of_Lotka–Volterra_2D_transformations.

Gasull, A. & Mañosa, V. [2020] "Periodic orbits of discrete and continuous dynamical systems via Poincaré–Miranda theorem," *Discr. Contin. Dyn. Syst. Ser. B* **25**, 651–670.

Guirao, J. L. G. & Lampart, M. [2008] "Transitivity of a Lotka–Volterra map," *Discr. Contin. Dyn. Syst. Ser. B* **9**, 75–82.

Jacobson, M. V. [1981] "Absolutely continuous invariant measures for one-parameter families of onedimensional maps," *Commun. Math. Phys.* **81**, 39–88.

Lai, Y. C. & Grebogi, C. [1996] "Noise-induced riddling in chaotic systems," *Phys. Rev. Lett.* **77**, 5047–5050.

Lai, Y. C., Grebogi, C., Yorke, J. A. & Venkataramani, S. C. [1996] "Riddling bifurcation in chaotic dynamical systems," *Phys. Rev. Lett.* **77**, 55–58.

Maistrenko, Y. L., Maistrenko, V. L., Popovich, A. & Mosekilde, E. [1998] "Transverse instability and riddled basins in a system of two coupled logistic maps," *Phys. Rev. E* **57**, 2713–2724.

Malicky, P. [2012] "Interior periodic points of a Lotka–Volterra map," *J. Diff. Eq. Appl.* **18**, 553–567.

Milnor, J. [1985] "On the concept of attractor," *Commun. Math. Phys.* **99**, 177–195.

Mira, C. [1987] *Chaotic Dynamics*: *From the One-Dimensional Endomorphism to the Two-Dimensional Diffeomorphism* (World Scientific, Singapore).

Mira, C., Gardini, L., Barugola, A. & Cathala, J. C. [1996] *Chaotic Dynamics in Two-Dimensional Noninvertible Maps* (World Scientific, Singapore).

Nagai, Y. & Lai, Y. C. [1997] "Periodic-orbit theory of the blowout bifurcation," *Phys. Rev. E* **56**, 4031–4041.

Ott, E. & Sommerer, J. C. [1994] "Blowout bifurcations: The occurrence of riddled basins and on-offintermittency," *Phys. Lett. A* **188**, 39–47.

Pecora, L. M. & Carroll, T. L. [1990] "Synchronization in chaotic systems," *Phys. Rev. Lett.* **64**, 821–824.

Pecora, L. M. & Carroll, T. L. [2015] "Synchronization of chaotic systems," *Chaos* **25**, 097611-1–13.

Sharkovsky, A. N. [1993] "Low dimensional dynamics," *Tagungsbericht 20/1993*, *Proc. Mathematisches Forschungsinstitut Oberwolfach*, 17.

Sharkovsky, A. N., Kolyada, S. F., Sivak, A. G. & Fedorenko, V. V. [1997] *Dynamics of One-Dimensional Maps* (Kluwer Academic, Boston).

Swirszcz, G. [1998] "On a certain map of the triangle," *Fundamenta Mathematicae* **155**, 45–57.

Thunberg, H. [2001] "Periodicity versus chaos in one-dimensional dynamics," *SIAM Rev.* **43**, 3–30.

Viana, R. L. & Grebogi, C. [2001] "Riddled basins and unstable dimension variability in chaotic systems with and without symmetry," *Int. J. Bifurcation and Chaos* **11**, 2689–2698.

Viana, R. L., De S. Pinto, S. E., Barbosa, J. R. R. & Grebogi, C. [2003] "Pseudo-deterministic chaotic systems," *Int. J. Bifurcation and Chaos* **13**, 3235–3253.